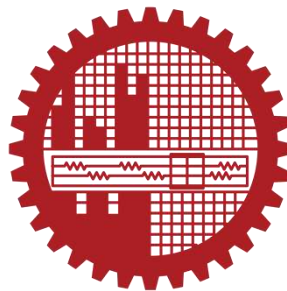


NUMERICAL ANALYSIS ON EFFICIENCY IMPROVEMENT OF SOLAR PHOTOVOLTAIC AND THERMAL HYBRID SYSTEM

by

Tasmin Akter Tripty
Student No. **0421092526**
Registration No. **0421092526**
Session: **April-2021**


**MASTER OF SCIENCE
IN
MATHEMATICS**




Department of MATHEMATICS
BANGLADESH UNIVERSITY OF ENGINEERING AND TECHNOLOGY, DHAKA
May, 2023

The thesis titled “NUMERICAL ANALYSIS ON EFFICIENCY IMPROVEMENT OF SOLAR PHOTOVOLTAIC AND THERMAL HYBRID SYSTEM”, submitted by Tasmin Akter Tripty, Student ID: 0421092526, Registration No. 0421092526, Session April-2021 has been accepted as satisfactory in partial fulfillment of the requirement for the degree of Master of Science in Mathematics on 23rd May, 2023.


Board of Examiners

1. 


Dr. Rehena Nasrin
Professor
Department of Mathematics
BUET, Dhaka-1000

**Chairman
(Supervisor)**
2. 


Dr. Nazma Parveen
Professor and Head
Department of Mathematics
BUET, Dhaka-1000

**Member
(Ex-Officio)**
3. 

Dr. Md. Abdul Alim
Professor
Department of Mathematics
BUET, Dhaka-1000

Member
4. 

Dr. Mohammed Forhad Uddin
Professor
Department of Mathematics
BUET, Dhaka-1000

Member
5. 

Dr. Md. Shajedul Karim
Professor
Department of Mathematics
SUST, Sylhet-3114

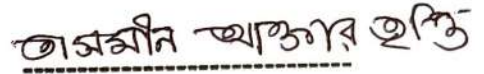
**Member
(External)**

Certificate of Research

This is to certify that the work presented in this thesis is carried out by the author under the supervision of **Dr. Rehana Nasrin**, Professor, Department of Mathematics, Bangladesh University of Engineering and Technology, Dhaka-1000.



Dr. Rehana Nasrin
Professor
Department of Mathematics
BUET, Dhaka-1000



Tasmin Akter Tripty
Student No. 0421092526

Candidate's Declaration

It is hereby declared that this thesis or any part of it has not been submitted elsewhere for the award of any degree or diploma.

তাসমিন আক্তার ত্রিপ্তি

Tasmin Akter Tripty

Student No. 0421092526

Registration No. 0421092526

Session: April-2021

May, 2023

This work is dedicated

to

My Mother, Father, Sister, Brother & Husband

Acknowledgement

I owe a deep depth to my supervisor, **Dr. Rehana Nasrin**, Professor, Department of Mathematics, Bangladesh University of Engineering and Technology (BUET) who restlessly supported me through the M.Sc. process. I would like to thank her for her invaluable contribution. Her understanding and expertise in the M.Sc. process is exceptional. Her contribution to this thesis, however, does not only encompass her role as an academic supervisor, but includes her ongoing friendship, care, and support on a personal level without which this journey may have never been completed.

I owe a favor to **Dr. Nazma Parveen**, Professor, and Head, Department of Mathematics, BUET, for her support in allowing me to use the departmental facilities in various stages of my work. I also thank the staff of the Department of Mathematics, BUET for being so helpful.

I would like to thank and express profound respect to **Dr. Md. Abdul Alim**, Professor, Department of Mathematics, BUET for his constant support, intuition, suggestions and continuous guidance throughout my thesis.

I want to offer my humble gratitude and profound respect to **Dr. Mohammed Forhad Uddin**, Professor, Department of Mathematics, BUET for his comments and constructive concept which helped me to better understand the issues of this thesis.

I would like to take the opportunity to thank **Dr. Md. Shajedul Karim**, an external member of the Board of Examiners and Professor, Department of Mathematics, Shahjalal University of Science and Technology. I am grateful to him for his valuable suggestions to improve this thesis work.

I wish to express my heartiest gratitude to all teachers, office staffs, and students, Department of Mathematics, BUET for giving me valuable ideas, suggestions, opinions, and physical facilities which helped me to complete the work smoothly.

Abstract

The depletion of traditional energy sources and the increasing demand for energy due to climate change has raised concerns among researchers worldwide. Solar energy, specifically photovoltaic thermal (PVT) systems, has the potential to become a major source of renewable energy for our planet. However, more research is necessary to optimize the performance, efficiency, and cost-effectiveness of PVT systems. This study examines a 3D solar photovoltaic and thermal hybrid system that utilizes air as a working fluid with six fins inside the heat exchanger. The heat exchanger's enclosure is constructed from corrosion-resistant stainless steel, and the heat exchanger's exposed surfaces are insulated with glass wool. The fins are manually circulated air, and the channels are made of aluminum, while an aluminum sheet with a thickness of 1 mm serves as the heat exchange component. The fins' top side is bent and firmly attached to the lower back floor of the solar photovoltaic (PV) panel to allow heat transfer from the PV panel to fins via the conduction technique. The study selected solar irradiation, inlet fluid mass flow rate, and inflow temperature between (250 - 500 W/m²), (0.015-0.5 Kg/s), and (10 - 40°C), respectively, based on Bangladesh's weather conditions. The study applied the finite element method (FEM) to solve heat transfer equations for PV layers, including glass, cells, fins, heat exchangers, and laminar flow equations for the fluid domain. The results indicate that a 50 W/m² increase in solar irradiation leads to a decrease of approximately 0.404% in overall efficiencies, while a 0.097 Kg/s increase in mass flow rate results in a 6.994% increase in overall efficiencies. Furthermore, a 5°C increase in inflow temperature leads to an overall efficiency increase of 0.33%. Hence, this study's findings could help researchers better comprehend air's properties as a heat exchanger in a developed design and they can be applied to government and commercial projects.

Contents

Acknowledgement	vi
Abstract.....	vii
Contents	viii
List of Tables	xiii
List of Figures.....	xiv
CHAPTER 1	16
INTRODUCTION	16
1.1 Overview	16
1.1.1 Heat transfer.....	17
1.1.2 Mechanism of heat transfer.....	17
1.1.3 Solar energy	19
1.1.4 Photovoltaic	20
1.1.5 Photovoltaic thermal.....	21
1.1.6 Solar irradiation.....	23
1.1.7 Mass flow rate.....	23
1.1.8 Inflow temperature	23
1.1.9 Electrical efficiency	23
1.1.10 Thermal efficiency.....	24
1.1.11 Total efficiency	24
1.2 Literature Review.....	25
1.3 Motivation.....	29
1.4 Objectives.....	29
1.5 Scope of Thesis	29
CHAPTER 2.....	31

NUMERICAL TECHNIQUES	31
2.1 Introduction	31
2.2 Finite Element Method	31
2.2.1 Discretization strategy.....	32
2.2.2 Galerkin’s weighted residual	33
2.2.2.1 Weighted residual method.....	33
2.2.2.2 Galerkin’s method.....	34
2.3 Physical Model.....	34
2.4 Mathematical Formulation	36
2.4.1 Boundary conditions	38
2.5 Computational Procedure	39
2.5.1 Mesh generation	39
2.5.2 Grid test	40
CHAPTER 3	41
RESULTS AND DISCUSSIONS.....	41
3.1 Data Analysis	41
3.2 Effect of Irradiation	42
3.3 Effect of Mass Flow Rate.....	45
3.4 Effect of Inflow Temperature	48
3.5 Cell Temperature	51
3.6 Electrical Power	52
3.7 Electrical Efficiency	54
3.8 Outlet Fluid Temperature	55
3.9 Thermal Energy	57
3.10 Thermal Efficiency.....	58

3.11 Overall Efficiency	60
3.12 Comparison	62
CHAPTER 4	64
CONCLUSIONS AND FUTURE RESEARCH	64
4.1 Conclusions	64
4.2 Future Research	66
References	67

Nomenclatures

A	Area of PVT surface (m^2)
C_p	Specific heat at constant pressure ($\text{J kg}^{-1}\text{K}^{-1}$)
E	Energy (W)
G	Solar irradiance (Wm^{-2})
k	Thermal conductivity ($\text{Wm}^{-1}\text{K}^{-1}$)
P	Pressure (kgms^{-2})
P_{sc}	Packing factor (%)
T	Temperature ($^{\circ}\text{C}$)
U	Heat transfer coefficient ($\text{Wm}^{-2}\text{K}^{-1}$)
u, v, w	Velocity components along x, y, z direction (ms^{-1})

Greek Symbols

α	Absorptivity
η	Efficiency (%)
ε	Emissivity
μ	Temperature coefficient
ν	kinematic viscosity of the fluid (m^2s^{-1})
ρ	Density of the fluid (kgm^{-3})
τ	Transmittivity

Subscripts

amb	Ambient
e	Electrical
f	fluid
g	Glass
ga	From glass to ambient
gtd	From glass to tedlar
in	Input
out	Output
r	Received
ref	Reference
sc	Solar cell
t	Thermal

td Tedlar

Abbreviation

FEM Finite Element Method

PV Photovoltaic

PCM Phase change material

PVT Photovoltaic thermal

2D Two dimensional

3D Three dimensional

List of Tables

Table 1.1:	Advantages of solar power.....	20
Table 1.2:	Applications of solar energy	20
Table 2.1:	The dimensions and properties of the PVT layers.....	35
Table 2.2:	Properties of PVT system.....	36
Table 2.3:	Grid sensitivity check at $G = 450 \text{ W/m}^2$, mass flow rate 0.054 kg/s , and inflow temperature 30°C	40
Table 3.1:	Bangladesh experiences monthly solar radiation	42
Table 3.2:	PVT cell temperature comparison with a few research	63
Table 4.1:	Conclusions from the present research	65

List of Figures

Figure 1.1:	Flow chart of heat transfer	18
Figure 1.2:	Solar energy technologies.....	19
Figure 1.3:	Photovoltaic (PV) systems.....	21
Figure 1.4:	Environmental impacts of Photovoltaic Thermal (PVT) system.....	22
Figure 2.1:	Usages of Finite Element Method (FEM)	32
Figure 2.2:	Flow chart of finite element discretization	33
Figure 2.3:	The schematic diagram of the PVT system	35
Figure 2.4:	Finite element meshing of a PVT system	40
Figure 3.1:	Surface temperature of PVT system for the variation of solar irradiation from 250 to 500 W/m ² at a mass flow rate of 0.054 Kg/s, and inflow temperature of 30°C.....	43
Figure 3.2:	Streamlines plot of PVT system for the variation of solar irradiation from 250 to 500 W/m ² at a mass flow rate of 0.054 Kg/s, and inflow temperature of 30°C	44
Figure 3.3:	Surface temperature of PVT system for the variation of mass flow rate from 0.015 to 0.535 Kg/s at irradiation level of 450 W/m ² , and inflow temperature of 30°C.....	46
Figure 3.4:	Streamlines plot of PVT system for the variation of mass flow rate from 0.015 to 0.535 Kg/s at irradiation level of 450 W/m ² , and inflow temperature of 30°C	47
Figure 3.5:	Surface temperature of PVT system for the variation of inflow temperature from 10°C to 40°C at 0.054 Kg/s, and irradiation level at 450 W/m ²	49
Figure 3.6:	Streamlines plot of PVT system for the variation of inflow temperature from 10°C to 40°C at 0.054 Kg/s, and irradiation level at 450 W/m ²	50

Figure 3.7: Solar cell temperature for the effect of (a) irradiance, (b) mass flow rate, (c) inflow temperature.....	52
Figure 3.8: Electrical power for the effect of (a) irradiance, (b) mass flow rate, (c) inflow temperature	53
Figure 3.9: Electrical efficiency for the effect of (a) irradiance, (b) mass flow rate, (c) inflow temperature.....	55
Figure 3.10: Outlet fluid temperature for the effect of (a) irradiance, (b) mass flow rate, (c) inflow temperature.....	56
Figure 3.11: Thermal energy for the effect of (a) irradiance, (b) mass flow rate, (c) inflow temperature	58
Figure 3.12: Thermal efficiency for the effect of (a) irradiance, (b) mass flow rate, (c) inflow temperature.....	59
Figure 3.13: Overall efficiency for the effect of (a) irradiance, (b) mass flow rate, (c) inflow temperature.....	61

CHAPTER 1

INTRODUCTION

1.1 Overview

One of the renewable energy sources with the fastest global growth is solar energy. Many nations are looking to solar energy as a safe and dependable replacement for fossil fuels due to growing worries about climate change, energy security, and economic prosperity. Solar energy and other renewable energy sources are playing a bigger role in the fight against climate change. With a capacity increase of 18% in 2020 alone, solar energy is the renewable energy source with the greatest rate of growth, according to the International Energy Agency (IEA). By 2021 and 2025, Bangladesh has set goals to use 10% and 15%, respectively, of renewable energy. As a result of government initiatives to encourage solar energy, such as a program to install 50,000 solar-powered irrigation pumps and a plan to install 6.5 million solar household systems by 2023, Bangladesh's installed capacity of solar energy has greatly expanded, reaching 725 MW in 2021. Using solar home systems, more than 4.5 million Bangladeshi people in rural areas now have access to power, enhancing their quality of life and enabling economic development.

A hybrid renewable energy technology known as a Photovoltaic and Thermal (PVT) system combines the production of thermal energy for heating water or air with the production of electricity using photovoltaic (PV) panels. PVT systems can create both heat and electricity from the same surface area, which can improve the system's total energy efficiency. The thermal component absorbs the heat from the sun's radiation that is not turned into energy by the PV cells, which convert sunlight into electricity. The excess heat from the PV cells is transferred to the absorber in a PVT system by a fluid that circulates between the PV cells and the absorber. The heat transfer fluid can then be utilized to generate additional thermal energy by heating water, a room, or the air. PVT systems are more effective at converting energy than typical PV systems because they can produce both electricity and heat at the same time while utilizing the same solar panel surface area. Moreover, PVT systems lower the total cost of solar energy because they take up less room than separate PV and thermal systems and do not require two different sets of supporting infrastructure. With a compound annual growth rate of 5.6% from 2019 to 2026, the size of the global solar PV market is anticipated to reach 476.56 GW by that

time. In addition, it is anticipated that between 2020 and 2027, the global market for solar thermal collectors would expand at a compound annual growth rate of 6.5%. Additionally, studies on PVT systems have revealed that, in comparison to conventional solar PV systems, they have the potential to increase solar energy production efficiency by up to 20%. This is because PVT systems are more effective at converting energy because they can produce both heat and electricity at the same time. PVT system research can also aid in overcoming the drawbacks of solar energy, including its intermittent nature and poor energy density. Research into solar energy with PVT systems is essential to the development of more effective and affordable technologies that can help to meet global energy demands while reducing greenhouse gas emissions in light of growing concerns about climate change and the need for a transition to clean energy.

The photovoltaic (PVT) system is a system that simultaneously generates thermal energy and electrical electricity. With the PVT system, one can obtain both electrical power and thermal energy thanks to the cooperation of a PV module and a thermal collector mechanism. This study examines the PVT system in Bangladesh under specific operating conditions numerically. Few related definitions and phenomena are given below:

1.1.1 Heat transfer

The fundamental rules of thermodynamics, which state that energy can only be transformed from one form to another and cannot be generated or destroyed, regulate how heat is transmitted. The temperature differential between two things or substances, the material qualities of the items or substances, and the area and distance between them all affect how quickly heat transfers between them. Mathematical models based on these fundamental concepts can be used to describe the three main mechanisms of heat transmission, conduction, convection, and radiation. Engineers and scientists can forecast and optimize heat transfer in a variety of applications, from the construction of effective heat exchangers to the study of atmospheric dynamics, thanks to these models and the study of heat transfer.

1.1.2 Mechanism of heat transfer

Common names for the specific mechanisms include convection, heat radiation, and conduction as shown in figure 1.1.

- ❖ **Conduction:** It involves the direct transmission of heat from atoms or molecules into another substance. In solids, heat is transferred through the motion of atoms or molecules, that in turn causes the vibration of nearby atoms or molecules. Heat is transmitted from one liquid or gas to another by atoms or molecules moving back and forth, which is typically a sluggish process.
- ❖ **Convection:** By moving fluid, such as air or liquid, heat is transferred. When a fluid is heated, convection happens because the fluid becomes less dense and rises. The fluid moves heat from one place to another as it rises by carrying heat energy with it.
- ❖ **Radiation:** It is the term used to describe the transfer of energy as electromagnetic radiation from its emission at a heated surface to its absorption on another surface.

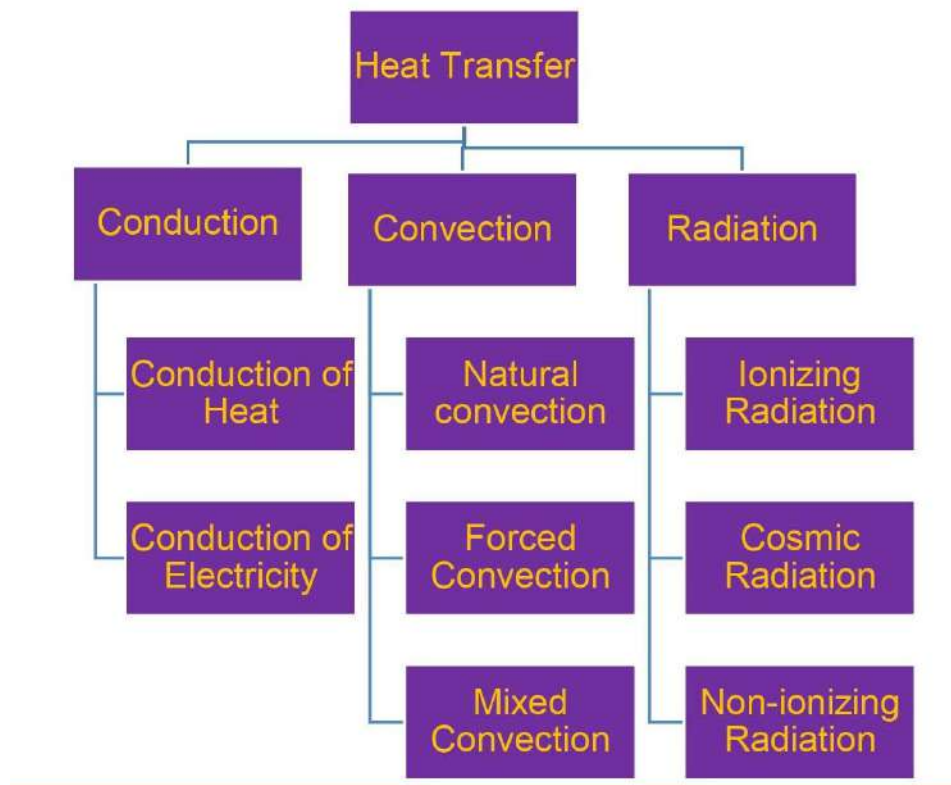


Figure 1.1: Flow chart of heat transfer

All of these activities, like heating a structure, a kettle of water, or a natural occurrence like a thunderstorm are typically involved in transferring heat. Overall, many physical and

engineering systems depend on heat transmission, which has significant effects on energy consumption, environmental sustainability, and the economy.

1.1.3 Solar energy

Solar energy is derived from the sun's radiation and is a renewable energy source. The installation of solar panels, which include photovoltaic cells that transform sunlight into electricity, is the first step in the generation of solar energy. Electrons in the cells are excited when sunlight strikes the solar panels, generating an electrical current. In order to power homes and businesses, this electricity can either be sent into the grid or stored in batteries for later use. In comparison to conventional fossil fuels, solar energy offers many advantages, including lowering greenhouse gas emissions and reducing reliance on non-renewable resources. Solar energy is a clean and renewable source of energy. A potential substitute for conventional energy sources in many regions of the world, solar energy is also getting more and more cost-effective and the growth is increasing every year. Some astonishing innovations in solar technology have shown in figure 1.2.

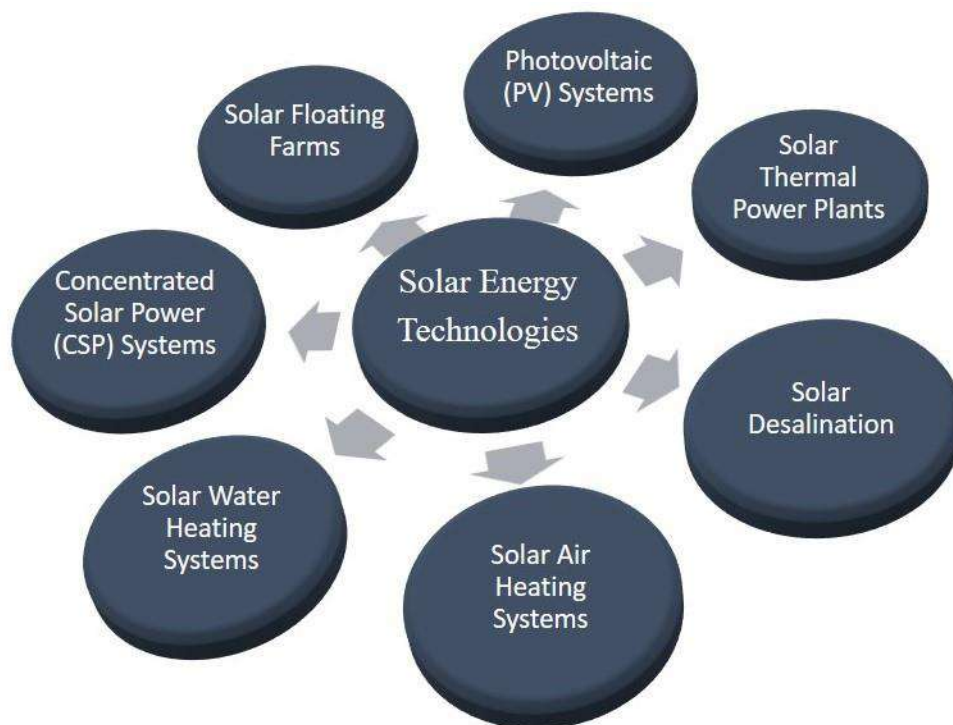


Figure 1.2: Solar energy technologies

The advantages and uses of solar energy are summarized in the table 1.1 and table 1.2 as follows:

Table 1.1: Advantages of solar power

Sustainable and Renewable	A renewable and sustainable form of energy that is not projected to run out anytime in the foreseeable future
Cost-Effective	Economical because they require little upkeep and have low running expenses
Environmentally responsible	It is a cleaner and more sustainable alternative to conventional fossil fuels because it emits no greenhouse gases
Independence from energy	Allows for the production of one's own electricity, fostering energy independence

Table 1.2: Applications of solar energy

Electricity for homes and businesses	For the purpose of generating power for residences and businesses, solar panels can be put on rooftops or in open spaces
Agriculture	Irrigation systems can be powered by solar energy, which is beneficial in places with low water availability
Catastrophe assistance	During natural catastrophes and other situations, portable solar panels can provide emergency power
Space exploration	For satellites and spacecraft, solar electricity is an essential source of power

1.1.4 Photovoltaic

Photovoltaic (PV) technology uses semiconducting materials to convert solar energy into direct current (DC) electricity. Electrons are excited when sunlight hits a photovoltaic cell, which causes them to flow through the material and create an electric current. PV cells are commonly built of silicon, but they can also be made of other materials such copper indium gallium selenide and cadmium telluride.

PV systems may produce electricity for buildings, offices, and even massive power plants. They can also be incorporated into construction materials like roofing shingles or building facades, as well as installed on rooftops or in open spaces. Grid-tied and off-grid PV systems are the two main varieties. Off-grid systems are stand-alone and frequently have batteries for energy

storage, whereas grid-tied systems are connected to the electrical grid and send any extra power back into the grid. Solar energy can be collected using a variety of photovoltaic (PV) systems, figure 1.3 shows a few of them.

The amount of sunlight available, the type and grade of materials utilized, the angle and orientation of the panels, and other elements all affect how efficient PV systems are. PV systems are becoming a more widely used option for renewable energy due to technological advancements that have enhanced efficiency and decreased costs.

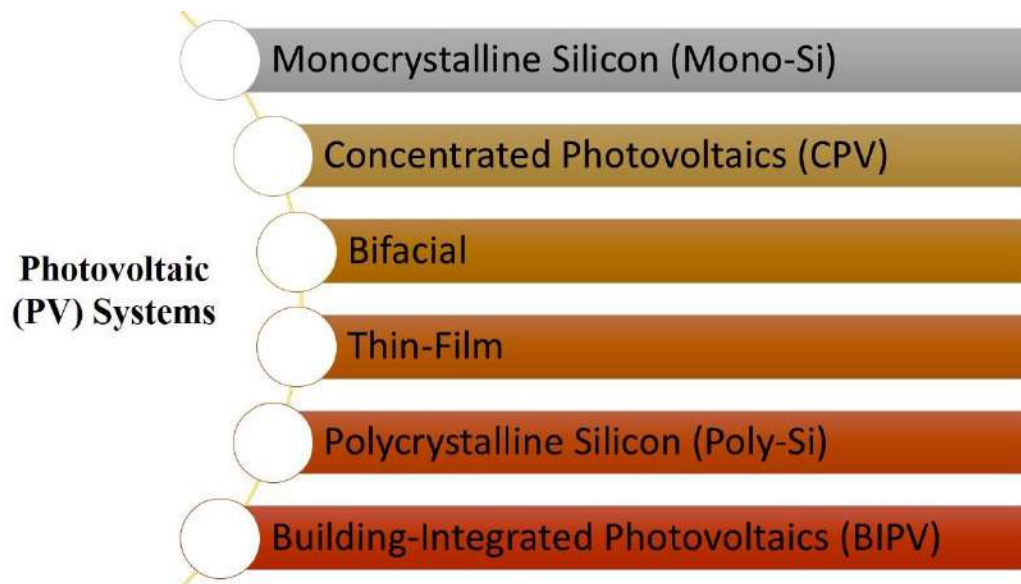


Figure 1.3: Photovoltaic (PV) systems

1.1.5 Photovoltaic thermal

A hybrid solar energy system, known as Photovoltaic Thermal (PVT), utilizes both solar thermal and photovoltaic (PV) techniques to produce heat and electricity simultaneously. A flat plate collector and a PV panel are integrated into the PVT system. A coating of an absorbent material that absorbs solar energy and transforms it into heat is applied to the flat plate collector, which is constructed of copper or aluminum. After passing through a heat exchanger, the heated fluid is transferred to a storage tank for later use. The PV panel, on the other hand, uses the sunshine it receives to produce power. It is possible to consume the electricity produced right away or to store it in batteries for later use. For those looking to produce both heat and electricity from the sun, the PVT system's mechanism enables the efficient utilization of solar thermal and

photovoltaic technologies. PVT system has very powerful impact on the environment, some of the environmental impacts have been shown in figure 1.4.

PVT systems were initially patented in the 1960s, giving them a more recent history than more established solar technologies like PV. PVT systems differ from PV systems in that they also generate heat, which can be utilized for space or water heating. PVT systems have a number of benefits over standalone PV and solar thermal systems, including increased energy efficiency, lower installation costs, and a more compact system design. The International Energy Agency predicts that from 2021 to 2026, the global market for PV systems will expand at a compound annual growth rate (CAGR) of 11%. The Asia-Pacific region will hold the highest share of the \$200 million PVT systems market in 2020, according to estimates. PVT systems, however, can be more difficult to build and install, and their performance can be impacted by things like temperature changes and shading.

To raise the effectiveness of PVT systems, lower their costs, and broaden their range of applications, research is crucial. PVT systems are still a young technology, therefore there is still much to learn about the best ways to build, run, and maintain them. With study, we can pinpoint and resolve technical issues that could be limiting their performance, such thermal losses. We can also investigate cutting-edge forms and substances that could improve their effectiveness and robustness. Research can also be used to determine the best uses for PVT systems and their potential economic and environmental advantages. Overall, PVT system research is essential to the development of renewable energy technologies and the realization of a sustainable energy future.

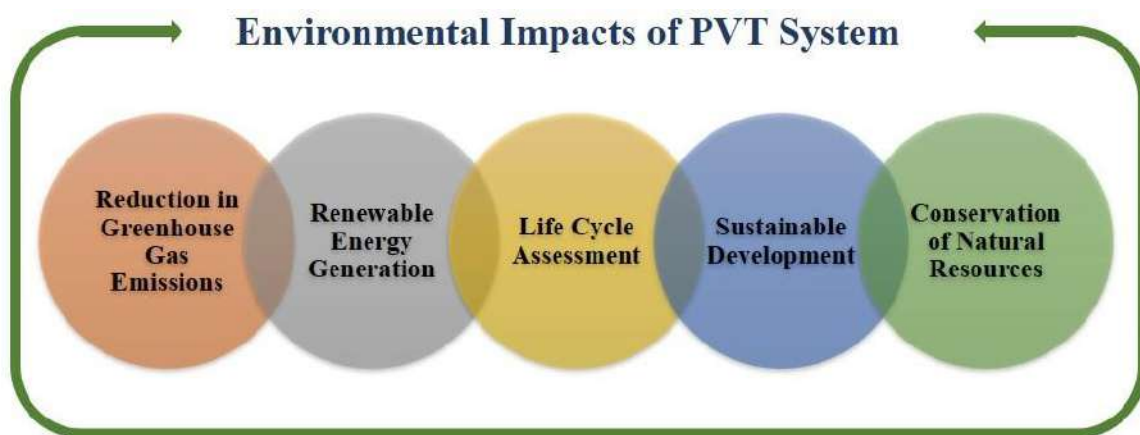


Figure 1.4: Environmental impacts of Photovoltaic Thermal (PVT) system

1.1.6 Solar irradiation

The amount of solar radiation that is received at a specific spot on the surface of the Earth is referred to as solar irradiation. It is commonly expressed in watts per square meter (W/m^2) and is subject to change depending on the latitude, time of day, and weather. Solar irradiation has a significant impact on the quantity of energy that can be produced from sunshine, making it an important consideration in the development and management of solar energy systems. Planning and maximizing the performance of solar energy systems therefore requires accurate measurements of sun irradiation. Reliable information on solar irradiation is obtained using methods like satellite-based monitoring and ground-based measuring stations.

1.1.7 Mass flow rate

The quantity of mass that moves through a certain site in relation to time is known as the mass flow rate. Usually, it is expressed in kilograms per second or pounds per hour. Mass flow rate is a crucial factor in thermodynamics and heat transfer because it affects how quickly heat and energy are transferred throughout a system. Size of the entrance, pressure differentials, and fluid characteristics are only a few examples of the variables that might affect the mass flow rate. While constructing and enhancing systems that include heat transfer, such as PVT systems, it is crucial to comprehend the mass flow rate.

1.1.8 Inflow temperature

The temperature of a fluid or medium as it enters a system or component is referred to as the inflow temperature. The inflow temperature can significantly affect how well a PVT (photovoltaic thermal) system performs. The system's thermal efficiency decreases as incoming temperature rises. To maximize the overall performance of the PVT system, it is crucial to keep the inflow temperature at a lower level. The longevity and dependability of the system can also be increased through proper inflow temperature monitoring and regulation.

1.1.9 Electrical efficiency

The efficiency with which a photovoltaic (PV) cell converts sunlight into energy is measured by its electrical output. It can be defined as the electrical power output to solar power incident ratio, represented as a percentage. Calculating electrical efficiency is as follows:

Electrical Efficiency = (Maximum power output / incident solar power) x 100%

The PV cell's current-voltage (IV) curve, which depicts the relationship between the current and voltage at various levels of solar intensity, is what determines the maximum power production. The quantity of solar energy that strikes the PV cell's surface area is known as incident solar power. However, getting high electrical efficiency demands managing a number of variables, including cell materials, design, and operating circumstances, which can impact the PV system's cost and performance.

1.1.10 Thermal efficiency

The ability of a system to transform heat energy into usable work or energy is referred to as thermal efficiency. It is the proportion between the energy a system produces and the thermal energy that is provided to it. The thermal efficiency equation is:

Thermal Efficiency = (Useful energy output / Energy input) x 100%

Thermal efficiency in the context of a PVT system refers to the system's capacity to transform solar energy into both electrical and thermal energy. High thermal efficiency makes the system more effective and efficient by allowing it to utilize a larger part of the solar energy that enters the system.

1.1.11 Total efficiency

Overall efficiency measures how well a PVT system performs overall in converting solar energy into useful forms of energy. It stands for the system's overall thermal and electrical efficiency. The equation for overall effectiveness is:

Total Efficiency = (Energy output / Energy input) x 100%

Energy Input is the total amount of energy a system receives from the sun, while Energy Output is the total amount of energy the system produces. The more solar radiation is converted into useful energy by the PVT system, the higher its overall efficiency. It's important to maximize the system's electrical and thermal efficiency if you want to reach high total efficiency.

1.2 Literature Review

Climate change and the exhaustion of conventional energy sources with the growing energy demand have caused concern among researchers worldwide. Renewable energy sources are a long-term alternative to our reliance on fossil fuels and reduce carbon emissions. A good alternative to dwindling and environmentally harmful fossil fuels is photovoltaic energy generating [1]. In a photovoltaic thermal (PVT) system, solar radiation is transformed into both electrical and thermal power. A 3D mathematical model of the photovoltaic thermal /phase change materials system was determined using the finite element method (FEM) by Ashikuzzaman et al. [2]. It has been noted that the average cell temperature rises with increasing irradiation intensity while employing paraffin as the PCM in the PVT module. A developed photovoltaic/thermal phase change system was designed by Hossain et al. [3] in which Lauric acid is taken as PCM and evaluated for its energy, exergy, and economic performance. In order to determine whether the suggested system may be commercialized, an economic study of it has also been done. An investigation on the performance of photovoltaic thermal collectors was conducted by Al-Waeli et al. [4] when operating a nanoparticle of SiC dispersed in water as a base fluid resulting that the suspension fluid should be re-mixed every 3 months to ensure that the thermal conductivity quality is not lost due to nanoparticle deposition. At a volume flow rate of 0.5 lit/min, adding 1% nanoparticles increases exergy efficiency by 0.45%, and increasing the flow rate from 0.5 to 4 lit/min decreases the efficiency by 2.03% [5].

Parametric analysis was performed to examine the effect of the phase change layer thickness on the thermal and electrical performance of the system. The findings show that magnesium oxide nanofluid has the lowest overall energy efficiency and multiwall carbon nanofluid has the greatest [6]. The use of Nanofluids in various energy systems is demonstrating that NFs typically have better heat transmission capabilities than pure fluids. NFs with metallic oxide were employed by the majority of the investigators [7]. A guideline had been introduced to minimize the impact of various environmental and operational factors to optimize the efficiency of solar photovoltaic cells. In humid environments, it has been discovered that dust deposition creates sticky, adhesive mud on PV cells, which worsens the problem by reducing power generation by up to 60–70% [8]. The current paper is a review of PVT (photovoltaic/thermal) investigations with a focus on research studies that consider environmental issues related to

PVT technology, such as PV cell material and heat transfer fluid. According to the analysis of the literature, the majority of studies focus on CO₂ emissions and EPBT (energy payback time) [9]. A new kind of heat exchanger was developed by Hossain et al. [10] for solar PVT hybrid systems to study performance in comparison to a PV solar panel that has identical specifications. According to the experiments, the open circuit voltage (V_{oc}) has improved on average by 0.97 V and has improved by 1.3 V in the highest cases. A 2.5 W boost in solar PV panel output power has also been made overall.

It was noted that a collector with cooling air is advised in emergency situations like floods and earthquakes or circumstances that only require the generation of electricity due to various factors, including the simplicity of the design, low cost, transfer speed, easy transportation, and lack of need for ancillary facilities [11]. By experimenting with various absorber arrangements, air flow patterns, and single- or double-pass designs, an air-based system has been created by Rukman et al. [12]. Hence an overview of various research and development of air-based PVT systems are conducted. Studies on the energy and exergy analyses of air-based PVT collectors from 2010 to 2018 are compiled. Air-based PV collectors have energy and exergy efficiencies that range from 31% to 94% and 8.7% to 18%, respectively. The first and second rules of thermodynamics are used to conduct exergy analysis [13]. A work had been conducted by Abed et al. [14] to evaluate a solar energy collector system's ability to heat water and air under actual operating circumstances resulting in the thermal efficiency of the hybrid solar collector system is often improved by a larger water flow rate, but the improvement diminished dramatically at higher air flow rates. Applications of PV/T technology include building integrated photovoltaic/thermal (BIPVT) collectors, PV-thermal/heat pump systems, water desalination, solar stills, solar cooling, and solar greenhouses are evaluated by Sultan et al. [15].

When a PV (photovoltaic) panel generates power, its temperature rises, but as it does so, its electrical efficiency falls. The remaining solar irradiance must be utilized in addition to maintaining an ideal temperature to maximize the PV efficiency [16]. Using Constantine (located in northeastern Algeria) as a case study, Ghellab et al. [17] presented energy balances for several nodes, including glazing, PV cells, absorbers, fluid, and back plates, while also considering transitory impacts. A work attempts to conduct an analysis of a single-glazed solar PVT air collector based on energy and exergy for the climatic conditions of Silchar, India. Maximum observed efficiencies for energy and exergy are 83% and 16.5%, respectively.

Thermal heat output makes up 60.7% of the overall useful heat production, while electrical heat output makes up the remaining portion [18]. The performance of a fin system integrated with a thin flat metallic sheet used to examine the performance of an air type single pass PV/T collector system (TFMS). The highest thermal efficiency and PV efficiency were found for four fins at 0.14 kg/s of mass flow rate and 700 W/m² of solar radiation, respectively, and were about 56.19% and 13.75% by Mojumder et al. [19]. The main variable in the production of photovoltaic energy is the level of radiation. Compared to conventional PV systems, photovoltaic/thermal systems are better at concentrating power in locations with high levels of radiation. With an optimal flow rate of 180 L/h, electrical and thermal energy increase from 197 to 983 W and 1165 to 5387 W respectively, for increasing irradiation from 1000 to 5000 W/m² were examined by Nasrin et al. [20]. Lamnatou et al. [21] give a general review of several PVT systems suitable for use in buildings, industries, etc. Its primary contribution is the classification of PVT configurations based on the working fluid's temperature.

The impact of sun irradiance on the thermal energy, electrical power, and overall efficiency of a three-dimensional PVT system is investigated by Zohora et. al. [22] using numerical modeling. According to numerical findings, the electrical, thermal, and total efficiency decrease by around 0.17, 0.67, and 0.83% for every 100 W/m² increase in solar irradiation. A 3D numerical system for a photovoltaic (PV) module was developed and solved by Nasrin et al. [23] using the software COMSOL Multiphysics, which is based on the FEM technique. In Rajshahi, where there is 209 W/m² of solar radiation, the highest electrical power value of 15.14 W is discovered, according to their studies. At a irradiation level of 189 W/m², Sylhet has the best electrical efficiency, measuring 12.85%. To enhance heat transmission and performance, Fayaz et al. [24] designed a unique thermal collector called PVT and PVT-PCM systems. The experimental research maintains the inlet water and ambient temperature at 27 °C and solar irradiation at 1000 W/m², which validates at various volume flow rates of 0.5 to 3LPM. In numerical and experimental situations, maximum electrical efficiency of PVT is 12.4% and 12.28%, respectively. Electrical performance for the PVT system is enhanced by 10.13 and 9.2%. A 3D numerical model of PVT with a novel baffle-based thermal collector system was created and solved by Nasrin et al. [25] using FEM. Different water-based nanofluids have been used, including Ag, Cu, and Al, as well as varying solid volume fractions up to 3% and varying inlet temperatures (20–40°C). The numerical results demonstrate that the

thermal performance of PVT systems driven by nanofluids improves with increasing solid volume fraction, and the ideal solid concentration is 2%. Indoor experimental research with varying mass flow rates of 30 to 120 L/h and a constant solar irradiation of 1000 W/m^2 has confirmed a numerical investigation by Fayaz et. al. [26]. At a flow rate of 120 L/h, the electrical efficiency of PV with nanofluid cooling is improved by roughly 10.72 and 12.25 percent in the numerical and experimental examples, respectively. For PVT systems run by water/MWCNT nanofluid, the percentage increase in thermal efficiency is found to be 5.62% numerically and 5.13% empirically when compared to water. At 1000 W/m^2 irradiation, a centrifugal pump-based active cooling for PVT system has been maintained; the numerical and experimental overall efficiencies are determined to be 89.2 and 87.65%, respectively [27]. To determine the power and energy of PV cells, high irradiation intensities between 1000 and 3000 W/m^2 have been examined by Nasrin et. al. [28]. When the irradiation level is increased from 1000 to 3000 W/m^2 , the overall energy increases by approximately 179.06%.

In light of the aforementioned arguments, this research intends to assess a new hybrid solar thermal system using the Finite Element Method (FEM). This system's overall performance will be enhanced by the addition of a heat exchanger and fins that direct air to pass waveform via channels. The method will be tested in real-world weather using meteorological data from Bangladesh. The overall goal of this research is to increase the utility of solar thermal systems and increase their effectiveness in a variety of applications.

1.3 Motivation

PVT (photovoltaic/thermal) system development and research is an intriguing and essential topic of study in the realm of sustainable energy. A PVT system uses PV cells to collect sunlight and transform it into electrical energy in order to generate heat and power. The heat exchanger is positioned behind the PV cells to receive the solar energy that was not fully converted into electricity. The thermal energy is subsequently transferred to a heat transfer fluid (HTF) that flows throughout the system by the heat exchanger. In order to heat water or air for a variety of uses, including space heating, water heating, or industrial processes, the HTF is then used.

Evaluation of PVT system performance in various environmental settings and design optimization for optimum performance are steps in the research process. We can fully utilize PVT technology and hasten the transition to a sustainable energy future by performing more study in this area. This represents a tremendous potential for scholars to make a big contribution to a greener and more sustainable world. It is an essential step in securing the availability of renewable energy sources for future generations.

1.4 Objectives

The goal of this study is to quantitatively analyze the solar photovoltaic thermal system's performance in Bangladesh under various operating circumstances. The following are the precise goals:

- i. To modify the 3D model of the solar photovoltaic and thermal hybrid system.
- ii. To solve the mathematical model using FEM.
- iii. To analyze the behavior of a hybrid system with a heat exchanger where the air will take direction to pass in waveform through the channel using fins.
- iv. To find out the condition of efficiency improvement.
- v. To compare the result with experimental/numerical published data.

1.5 Scope of Thesis

The four chapters that make up this thesis each provide a brief summary of the most recent numerical analysis of the electrical and thermal power and efficiency of a PVT system:

In Chapter 1, a summary of the project's objectives is provided. This chapter also provides a review of earlier research on the electrical and thermal power of several solar PVT system types operating in various environments in various countries that is pertinent to the current investigation. Different components of earlier studies have been specifically acknowledged. This chapter also covers the most recent research as well as its drivers.

In Chapter 2, the numerical method is adequately explained. Additionally, a detailed description of the structural design of a PV module (E310P(S)-011 of EPV brand, Malaysia) is provided. A PVT system has been demonstrated by inserting a thermal system with this PV module. The physical and material characteristics of the PVT system, as well as its schematic representation, are also displayed. The 3D numerical analysis of this PVT system. The proper boundary conditions are mathematically specified for each layer of the PVT system. Additionally, a numerical computational strategy that involved grid testing and mesh creation is shown.

In Chapter 3, it presents the findings and discussions. PVT's surface temperature and streamlines are used to visualize the numerical results inside the fluid domain. The solar cell and PVT outlet temperatures, electrical and thermal energy, and electrical and thermal efficiency are determined for each parameter variation. Under various operational conditions, the performance of the PVT system in Bangladesh is calculated. Finally, a comparison between previously released results and the current numerical results is done.

In Chapter 4, several important factors are covered when selecting whether to use the PVT system. The paper's final remarks and recommendations for further research are also presented logically.

NUMERICAL TECHNIQUES

2.1 Introduction

Scientific and technical research now relies heavily on numerical approaches because they make it possible to simulate and analyze complicated systems that would otherwise be difficult or impossible to examine experimentally. These methods model and resolve issues ranging from fluid dynamics and heat transfer to electromagnetics and structural analysis using mathematical algorithms and computer simulations. Numerous problems may now be studied thanks to the application of numerical approaches, which has also helped progress industries including renewable energy, automotive engineering, and aerospace. Numerical methods are used to model and optimize photovoltaic and solar thermal systems in the field of solar energy, which helps to increase their effectiveness and lower their cost. Numerical simulations are becoming a more important tool for study and design as their accuracy and speed increase due to computer hardware and software improvements.

2.2 Finite Element Method

German mathematician R. Courant was the first to propose the idea of variational techniques for resolving differential equations. Engineers and mathematicians started using the Finite Element Method (FEM) to tackle a wide range of issues in a variety of disciplines, including civil engineering, mechanical engineering, and fluid dynamics, in the late 1950s and early 1960s. When digital computers first appeared in the 1960s and 1970s, the FEM quickly gained popularity as a tool for tackling challenging engineering and scientific issues.

A popular computational method for resolving engineering issues involving complicated geometries and boundary conditions is the finite element method (FEM). The FEM separates a problem area into smaller, easier subdomains, or elements, and then uses numerical techniques to solve the problem in each element. The ultimate solution for the full domain is then created by combining the results of all the elements' solutions. Numerous disciplines have discovered

uses for the FEM, some of them have shown in figure 2.1. It is especially helpful when there are no practical analytical solutions or when the issue is too complex to be resolved using conventional means. This technique may now be more easily applied to real-world engineering issues via FEM software packages, which makes it a crucial tool for contemporary engineering design and analysis. Examples include the Galerkin method, the discontinuous Galerkin method, mixed techniques, and further variational formulations.

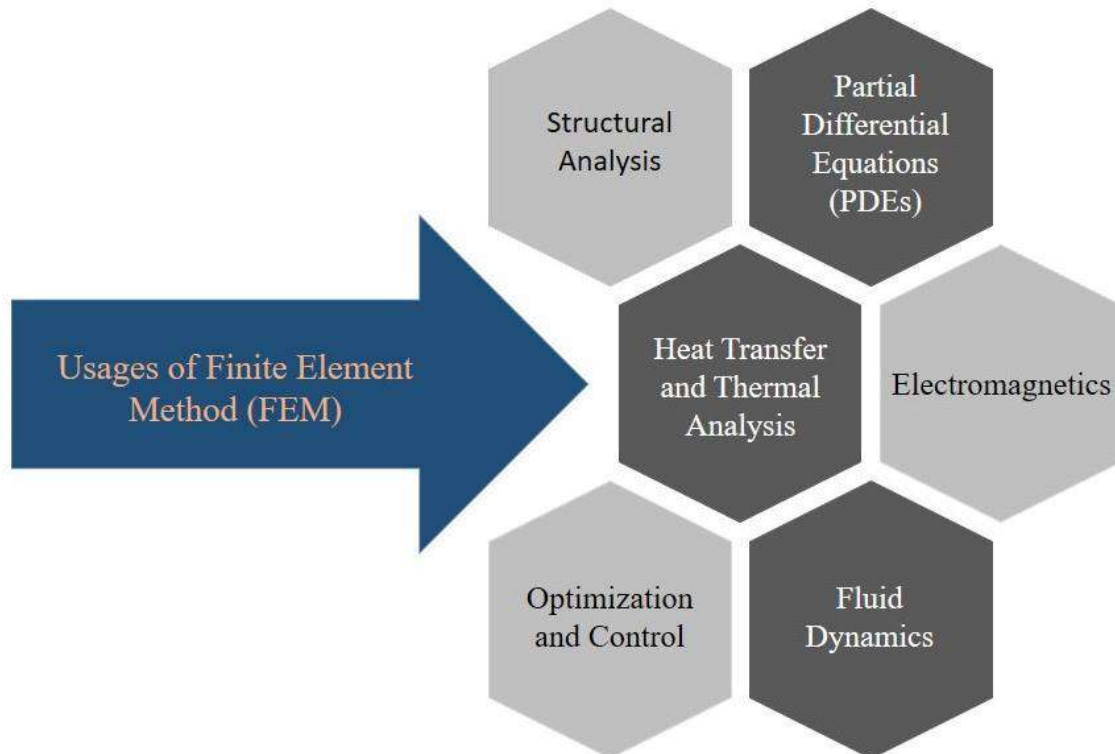


Figure 2.1: Usages of Finite Element Method (FEM)

2.2.1 Discretization strategy

In finite element analysis, discretization of an element refers to the act of breaking the body into an equivalent number of finite elements connected to nodes. Figure 2.2, which is provided in next page, illustrates the discretization step in a FEM model.

Overall, because it directly affects the precision and computational effectiveness of the numerical solution, the discretization approach is an integral component of the finite element method.

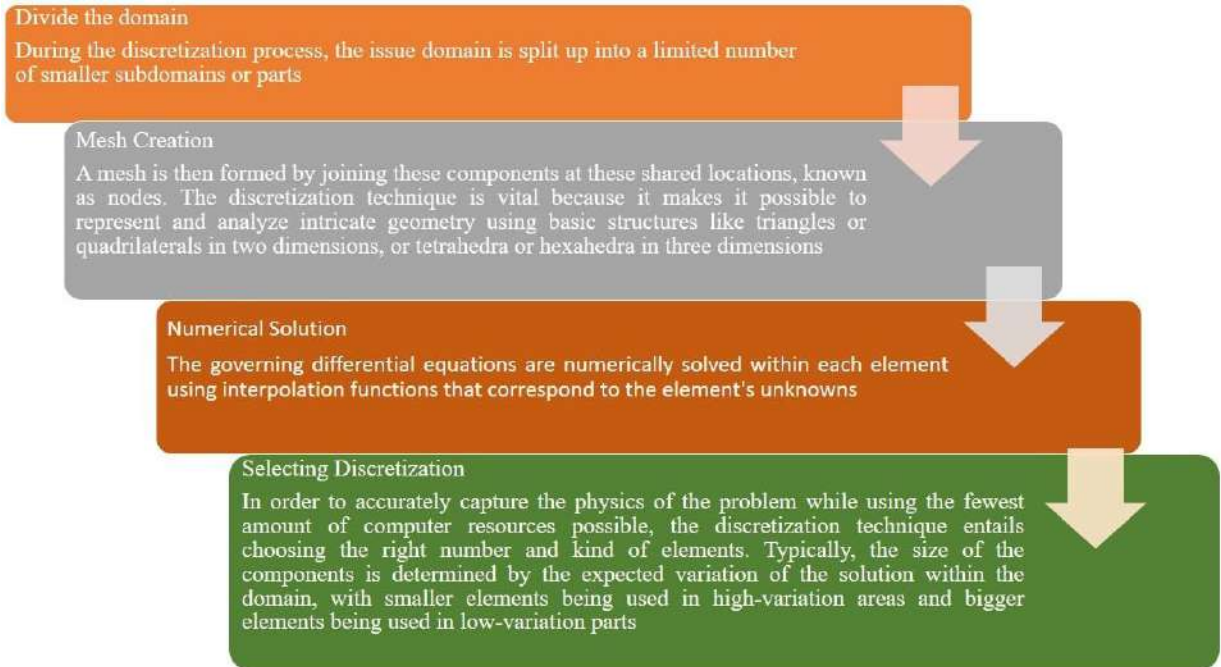


Figure 2.2: Flow chart of finite element discretization

2.2.2 Galerkin's weighted residual

A numerical approach is utilized to solve differential equations is the Galerkin weighted residual method. Choosing weights to minimize the residual, the discrepancy between the differential equation and the approximate solution entails first approximating the differential equation's solution using a linear combination of basis functions.

2.2.2.1 Weighted residual method

Using a finite collection of basis functions to approximate the solution, the Weighted Residual Method is a numerical method for solving partial differential equations. The governing equation is multiplied by a weighting function, the domain is integrated, and finally the boundary conditions are applied. The basis functions and weighting functions for the approach must be specified, and they can be selected based on how the answer is anticipated to behave. The basis and weighting functions, as well as the discretization mesh size, are all factors that affect the

method's accuracy. It's common practice to employ the Weighted Residual Method to address many engineering issues.

2.2.2.2 Galerkin's method

Popular numerical methods for solving partial differential equations include Galerkin's approach. A residual function that results from the weak version of the governing equation must be minimized. A finite set of basis functions that meet the problem's boundary conditions are used to approximate the solution in this method. Usually, polynomial functions are used as these foundation functions. The benefit of using Galerkin's method is that the solution is accurate and steady. The technique is frequently used to solve issues with heat transfer, fluid mechanics, and structures.

2.3 Physical Model

The two-dimensional sketches of the PV module and the heat exchanger are displayed along the zx and yx directions, respectively, in figure 2.3's schematic diagram of the PVT system, which was adapted from [1, 2, 15, 20]. For the purpose of the current numerical investigation, the geometrical and physical characteristics of the PV module (E310P(S)-011 of EPV brand, Malaysia) were used. The module comprises 72 (6*12) polycrystalline solar cells with a size of 156*156 mm, a maximum power of 295 W, a weight of 22 kg, a dimension of 1984*997*42 mm, a maximum power voltage of 30.6 V, a maximum power current of 8.17 A, an open-circuit voltage of 45.7 V, and a maximum short circuit current of 8.92 A. The ethylenevinyl acetate (EVA)-1 layer, polycrystalline silicon layer, EVA-2 layer, and Tedlar polyvinyl fluoride (PVF) layer are the main layers used to create PV. Glass (3 mm), polycrystalline cells (0.1 mm), EVA (0.8 mm), and tedlar (0.05 mm) make up the thickness of PV surfaces. By applying thermal paste to the PV bottom surface, a rectangle-shaped box-shaped heat exchanger will be attached for cooling purposes. A new design will be created employing six aluminum sheets with 1 mm thick fins (as a heat exchange material) inside the heat exchanger to obtain the most thermal energy possible. The heat exchanger's dimensions are 2000*1000*10 mm, the air input-output dimensions are 5*50*10 mm, and the flow fins are 181.8181818*950*10 mm. Table 2.1 lists the physical characteristics of the PVT module's several levels. Table 2.2 lists other characteristics of the photovoltaic thermal system.

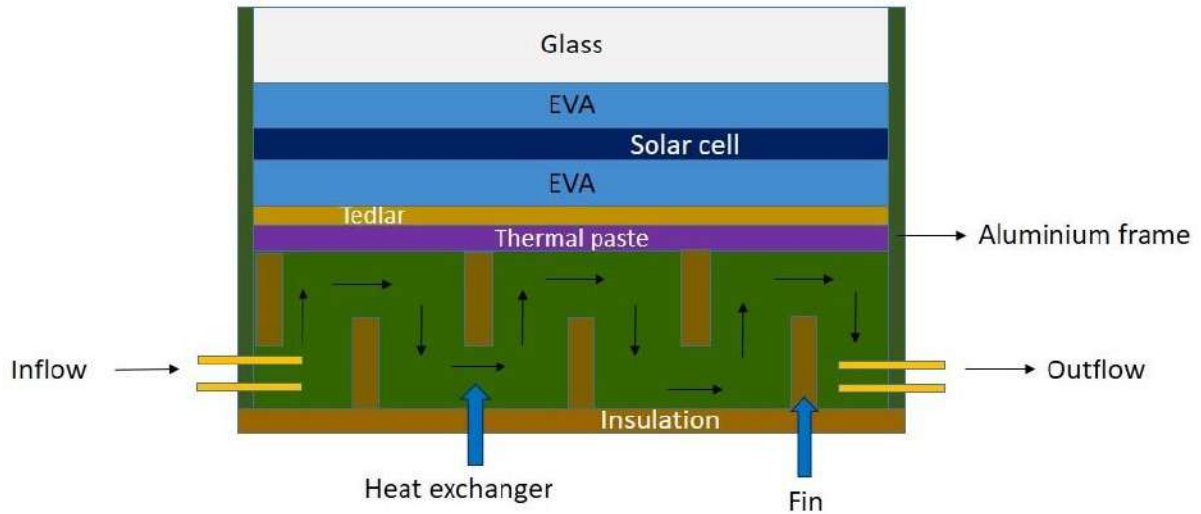


Figure 2.3: The schematic diagram of the PVT system [1, 2, 15, 20]

Table 2.1: The dimensions and properties of the PVT layers [1, 20, 22, 24, 25, 26, 27, 28, 29]

PVT components	Dimension (m)	Density ρ [kg /m ³]	Specific heat C_p [J/(kg. K)]	Thermal conductivity k [W/(m.K)]
Glass	2×1×0.003	2450	500	2
EVA	2×1×0.0008	950	2090	0.311
Polycrystalline cell	1.75×1×0.0001	2329	700	148
Tedlar	2×1×0.00005	1200	1250	0.15
Thermal paste	2×1×0.0003	2600	700	1.9
Heat exchanger	2×1×0.01	1.164	1007	0.02588
Air inlet-outlet	0.005×0.05×0.01	1.164	1007	0.02588
Fins	0.18×0.95×0.01	237	900	2700
Fluid	2×1×0.01(fluid region)	1.164	1007	0.02588

Table 2.2: Properties of PVT system [20, 22, 23, 25, 26, 27, 28, 29]

Properties	Value
Glass transmittivity, τ_g	0.96
Emissivity of glass, ε_g	0.04
Solar cell absorptivity, α_{sc}	0.9
Tedlar absorptivity, α_{td}	0.5
Reference efficiency of PV cell, η_{sc} (%)	0.15
PV temperature coefficient, μ_{SC}	0.0045
Ambient temperature, T_{amb} (°C)	30
Fluid input temperature, T_{in} (°C)	30
Reference temperature, T_r (°C)	25
Packing factor, P_{sc}	20%
Area of each cell (m ²)	0.156*0.156
PVT area, A (m ²)	2
Number of cell	6*12
Heat transfer coefficient inside PV layers, U_t (W/m ² K)	150
Heat transfer coefficient from tedlar to heat exchanger, U_{td} (W/m ² K)	77
Heat transfer coefficient from heat exchanger to ambient, U_{hea} (W/m ² K)	5.84
Heat transfer coefficient from heat exchanger to air, U_{he} (W/m ² K)	66

2.4 Mathematical Formulation

The flow is modeled mathematically as laminar, incompressible, and without viscous dissipation. It is believed that the gravitational force is insignificant, and fluid is moving through the heat exchanger at the inlet velocity. Conduction heat transfer, in which thermal energy is carried through the body by vibrating particles, is usually thought to be the only method of heat transmission in the solid domains of the PVT system. Other assumptions for this numerical simulation can be found in Nasrin et al. [20] and Zohora et al. [22], which do not include the wind speed. According to [20, 22], the heat transfer equations for PV layers and the equations for laminar flow in the fluid domain of a PVT system are as follows:

For the glass

$$\begin{aligned}
 -\left(\frac{k}{\rho C_p}\right)_g \left(\frac{\partial^2 T_g}{\partial x^2} + \frac{\partial^2 T_g}{\partial y^2} + \frac{\partial^2 T_g}{\partial z^2}\right) \\
 = \alpha_g \tau_g G - U_{ga}(T_g - T_{amb}) - \epsilon_g \sigma (T_g^4 - T_s^4) - U_t(T_g - T_{sc})
 \end{aligned} \tag{2.1}$$

For the cell

$$-\left(\frac{k}{\rho C_p}\right)_{sc} \left(\frac{\partial^2 T_{sc}}{\partial x^2} + \frac{\partial^2 T_{sc}}{\partial y^2} + \frac{\partial^2 T_{sc}}{\partial z^2}\right) = U_t(T_g - T_{sc}) - E_e - U_t(T_{sc} - T_{td}) \tag{2.2}$$

For the tedlar

$$-\left(\frac{k}{\rho C_p}\right)_{td} \left(\frac{\partial^2 T_{td}}{\partial x^2} + \frac{\partial^2 T_{td}}{\partial y^2} + \frac{\partial^2 T_{td}}{\partial z^2}\right) = U_t(T_{sc} - T_{td}) - U_{td}(T_{td} - T_{he}) \tag{2.3}$$

For the heat exchanger

$$-\left(\frac{k}{\rho C_p}\right)_{he} \left(\frac{\partial^2 T_{he}}{\partial x^2} + \frac{\partial^2 T_{he}}{\partial y^2} + \frac{\partial^2 T_{he}}{\partial z^2}\right) = U_{td}(T_{td} - T_{he}) - U_{he}(T_{he} - T_f) \tag{2.4}$$

For the fluid domain

$$\frac{\partial u}{\partial x} + \frac{\partial v}{\partial y} + \frac{\partial w}{\partial z} = 0 \tag{2.5}$$

$$\rho_f \left(u \frac{\partial u}{\partial x} + v \frac{\partial u}{\partial y} + w \frac{\partial u}{\partial z}\right) = -\frac{\partial P}{\partial x} + \nu_f \left(\frac{\partial^2 u}{\partial x^2} + \frac{\partial^2 u}{\partial y^2} + \frac{\partial^2 u}{\partial z^2}\right) \tag{2.6}$$

$$\rho_f \left(u \frac{\partial v}{\partial x} + v \frac{\partial v}{\partial y} + w \frac{\partial v}{\partial z}\right) = -\frac{\partial P}{\partial y} + \nu_f \left(\frac{\partial^2 v}{\partial x^2} + \frac{\partial^2 v}{\partial y^2} + \frac{\partial^2 v}{\partial z^2}\right) \tag{2.7}$$

$$\rho_f \left(u \frac{\partial w}{\partial x} + v \frac{\partial w}{\partial y} + w \frac{\partial w}{\partial z}\right) = -\frac{\partial P}{\partial z} + \nu_f \left(\frac{\partial^2 w}{\partial x^2} + \frac{\partial^2 w}{\partial y^2} + \frac{\partial^2 w}{\partial z^2}\right) \tag{2.8}$$

$$(\rho_f C_{pf}) \left(u \frac{\partial T_f}{\partial x} + v \frac{\partial T_f}{\partial y} + w \frac{\partial T_f}{\partial z}\right) = k_f \left(\frac{\partial^2 T_f}{\partial x^2} + \frac{\partial^2 T_f}{\partial y^2} + \frac{\partial^2 T_f}{\partial z^2}\right) \tag{2.9}$$

Here $\sigma = 5.670367 \times 10^{-8} \text{ Wm}^{-2}\text{K}^{-4}$ is Stefan-Boltzmann constant, $T_s = 0.0552T_{amb}^{1.5}$ is the sky temperature. Also ρ_f , k_f , C_{pf} , and ν_f are the density, thermal conductivity, specific heat at constant pressure, and dynamic viscosity of the fluid, respectively.

The amount of total received energy by the PVT system can be calculated by:

$$E_r = \tau_g \alpha_{sc} P_{sc} GA \quad (2.10)$$

Solar cell temperature can be calculated from the equation:

$$T_{sc} = \frac{P_{sc} G (\tau_g \alpha_{sc} - \eta_{sc}) + (U_{ga} T_{amb} + U_{gtd} T_{td})}{(U_{ga} + U_{gtd})} \quad (2.11)$$

The following equations can be used to compute the output electrical power and thermal energy of the PVT module:

$$E_e = \eta_{sc} P_{sc} \tau_g \alpha_{sc} GA [1 - \mu_{sc} (T_{sc} - T_r)] \quad (2.12)$$

$$\text{and } E_t = m C_p [T_{out} - T_{in}] \quad (2.13)$$

The following relationships can be used to calculate the instantaneous electrical, thermal, and total efficiency of the PVT system, respectively:

$$\eta_e = \frac{\text{Produced electrical power}}{\text{Total received energy}} = \frac{E_e}{E_r} \quad (2.14)$$

$$\eta_t = \frac{\text{Generated thermal energy}}{\text{Total received energy}} = \frac{E_t}{E_r} \quad (2.15)$$

$$\eta_o = \eta_e + \eta_t = \frac{E_e + E_t}{E_r} \quad (2.16)$$

2.4.1 Boundary conditions

Based on the physics of the issue, the proper boundary conditions were utilized in the computational domain. According to Nasrin et al. [20] and Zohora et al. [22], the following describes the boundary conditions of the numerical model:

$$\text{For side surfaces of PVT: } -n \cdot (k \nabla T) = 0 \quad (2.17)$$

$$\text{For the top of the glass surface: inward heat flux: } k_g \frac{\partial T_g}{\partial z} = G \quad (2.18)$$

$$\text{For solid boundaries of fluid domain: } u = v = w = 0 \quad (2.19)$$

$$\text{For the solid-fluid interface: } k_f \left(\frac{\partial T}{\partial n} \right)_f = k_{he} \left(\frac{\partial T}{\partial n} \right)_{he}, T_f = T_{he} \quad (2.20)$$

$$\text{For inlet: } T = T_{in}, u = U_{in}, v = 0, w = 0 \quad (2.21)$$

$$\text{For outlet: } P = 0 \quad (2.22)$$

where n is the distance along x or y or z directions, acting normal to the surface.

2.5 Computational Procedure

For the purpose of the current simulation, the 3D numerical model of PVT, which is the system of nonlinear PDEs (2.1) - (2.9), is solved using the finite element method (FEM) and Galerkin's weighted residual methodology [30]. The mass conservation, energy conservation, and momentum equations play a very important role to know the temperature of the solar cell (T_{sc}), output fluid (T_{out}), the pressure (P), and velocity (u, v, w) of fluid in the PVT system. After being transformed into linear algebraic equations, the nonlinear equations are solved. The convergence of solutions will be assumed when the relative error for each variable between subsequent iterations is reported below the convergence criteria (10^{-4}).

2.5.1 Mesh generation

The finite element meshing of a PVT module's computational domain is shown in figure 2.4. In this numerical model, the subdomain and boundary elements are represented by free tetrahedral and triangular forms, respectively. Tetrahedral and triangular elements use ten and six nodes, respectively. The simulation program includes a variety of mesh types.

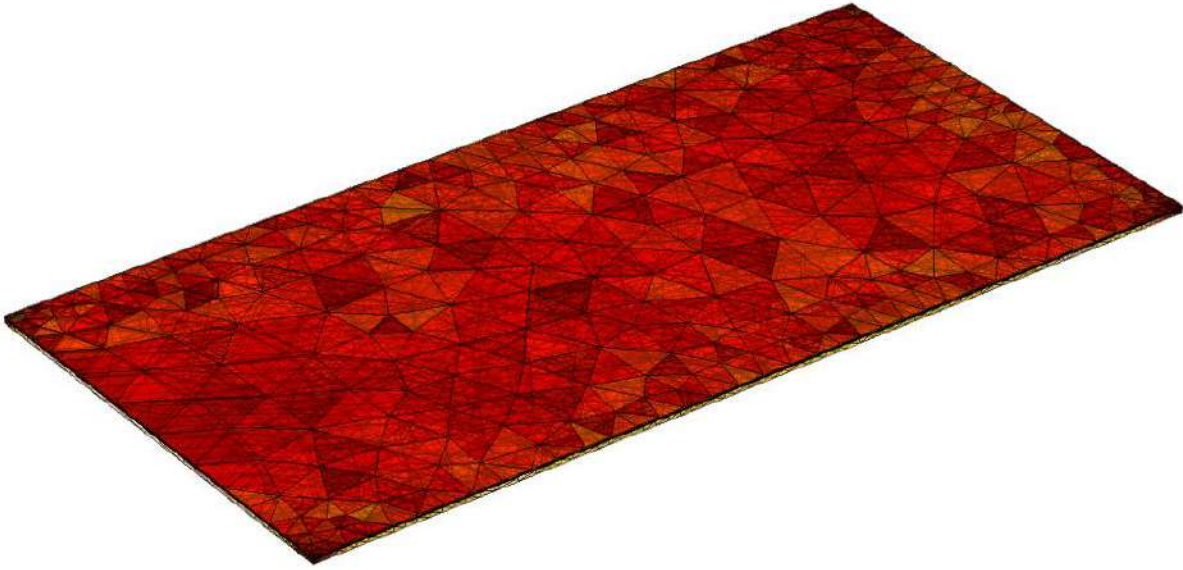


Figure 2.4: Finite element meshing of a PVT system

2.5.2 Grid test

The PVT model was grid tested with an irradiation level of 450 W/m^2 and a mass flow rate of 0.109 kg/s . Elements 22,121; 45,322; 75,319; 1,23,590; and 2,48,400 are used to check several forms of non-uniform grid systems. Monitoring metrics include cell temperature and the temperature of the outflow fluid. Normal and fine meshing did not significantly differ in the values of cell and outlet temperatures, but the timing was inadequate. Hence, considering the non-uniform grid system of 1,23,590 elements for normal meshing type is preferred for the computation. The results of the grid test are displayed in table 2.3.

Table 2.3: Grid sensitivity check at $G = 450 \text{ W/m}^2$, mass flow rate 0.054 kg/s , and inflow temperature 30°C

No. of element	22121	45322	75319	123590	248400
$T_{sc}(\text{C})$	44.48	44.73	44.83	45.13	45.134
$T_{out}(\text{C})$	38.49	38.76	38.97	39.52	39.523
Time (s)	105	217	337	562	812

RESULTS AND DISCUSSIONS

3.1 Data Analysis

As it lays the foundation for the offered findings, the introduction of the results and discussions of this thesis is a crucial step in the research process. The methodology used to gather and evaluate the data is briefly described in this part, along with the research questions and objectives. The main goal is to summarize the most important facts and conclusions from the analysis. The possibility for further study as well as a discussion of their ramifications are also included. The conversation is set within the framework of the body of knowledge already available on solar energy and related subjects. This section's main objective is to thoroughly examine the research findings and show how they advance our understanding of solar energy.

Bangladesh is ideally located for solar energy because of its location in a region with lots of sunlight. However, the nation's capacity to utilize this power source is hampered by a lack of access to necessary technology. Bangladesh receives an average of 5 KWh/m² of irradiation each month despite having a total area of 1.49E+11 m² and a tropical environment. Many types of solar energy equipment have undergone considerable developments in recent decades; some have even entered the commercial stage. Table 3.1 from Nasrin et al. [23, 31] displays the monthly irradiation (KWh/ m²) at several sites around Bangladesh. In May, solar radiation is at its maximum, while it is at its lowest in December. Dhaka, Rajshahi, Sylhet, Chittagong, Barisal, and Khulna each have annual average irradiation values of 197, 209, 189, 192, 196, and 202 W/m², respectively.

It is vital to produce data once the steady-state condition has been established in order to obtain an accurate prediction of the PVT system yield. Instead of the more time-consuming 3D dynamic model, the 3D steady-state model has been adopted in the current study. The effect of high sun irradiation on the thermal and electrical power and efficiency of PVT modules is investigated using numerical simulation. The following ranges of values for solar irradiation, intake fluid mass flow rate, and inflow temperature are considered: 250 - 500 W/m², 0.015-0.535 kg/s, and 10 - 40°C. The results of the various examples are shown in the following

sections:

Table 3.1: Bangladesh experiences monthly solar radiation [23, 31]

No. of month in year	Sylhet	Chittagong	Khulna	Rajshahi	Barisal	Dhaka
01	4	4.01	4.25	3.96	4.17	4.03
02	4.63	4.69	4.85	4.47	4.81	4.78
03	5.2	5.68	4.5	5.88	5.30	5.33
4	5.24	5.87	6.23	6.24	5.94	5.71
05	5.37	6.02	6.09	6.17	5.75	5.71
06	4.53	5.26	5.12	5.25	4.39	4.8
07	4.14	4.34	4.81	4.79	4.2	4.41
08	4.56	4.84	4.93	5.16	4.42	4.82
09	4.07	4.67	4.57	4.96	4.48	4.41
10	4.61	4.65	4.68	4.88	4.71	4.61
11	4.32	4.35	4.24	4.42	4.35	4.27
12	3.85	3.87	3.97	3.82	3.95	3.92
Average irradiation (KWh/m ² /day)	4.54	4.56	4.85	5	4.71	4.73
Average irradiation (W/m ²)	189	192	202	209	196	197

Based on the above weather conditions of Bangladesh, in this research, we use different solar irradiation (250 - 500 W/m²), mass flow rate (0.015 - 0.535 kg/s), and inflow temperature (10 - 40°C). We want to analyze mentioned parameter effects on cell temperature, electrical power, electrical efficiency, outlet temperature, thermal energy, thermal efficiency, and overall efficiency. In the following section, we will discuss these terms elaborately.

3.2 Effect of Irradiation

Figure 3.1 displays the relationship between surface temperature and solar irradiation as it relates to temperature. Solar irradiation values between 250 W/m² to 500 W/m² are taken into consideration, with an inflow temperature of 30°C and a mass flow rate of 0.054 Kg/s. surface

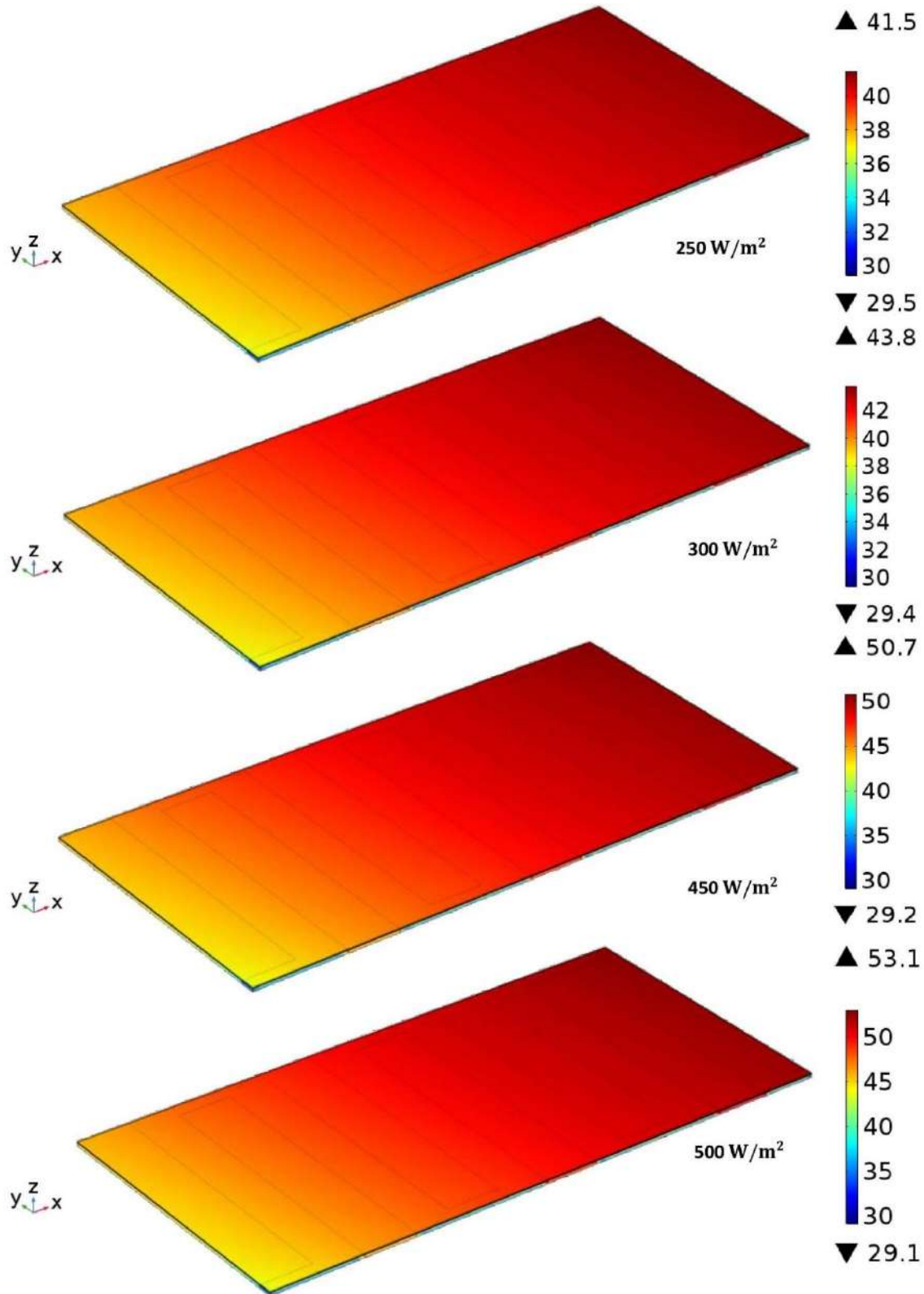


Figure 3.1: Surface temperature of PVT system for the variation of solar irradiation from 250 to 500 W/m^2 at a mass flow rate of 0.054 Kg/s and inflow temperature of 30°C

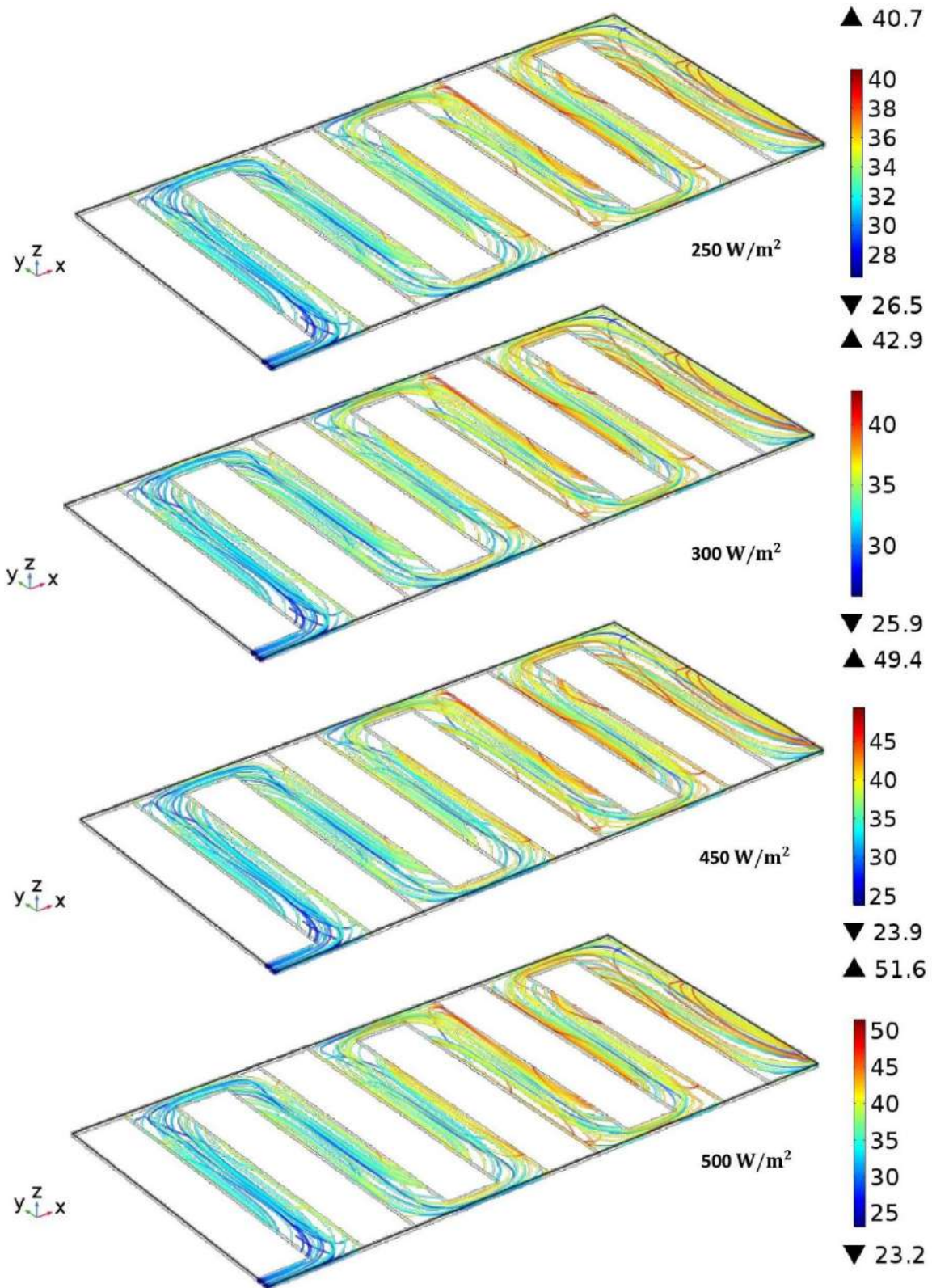


Figure 3.2: Streamlines plot of PVT system for the variation of solar irradiation from 250 to 500 W/m² at a mass flow rate of 0.054 Kg/s, and inflow temperature of 30°C

temperatures range from 29.5 to 41.5°C for solar irradiation of 250 W/m², 29.4 to 43.8°C for solar irradiation of 300 W/m², 29.3 to 46.1°C for solar irradiation of 350 W/m², 29.2 to 48.4°C for solar irradiation of 400 W/m², 29.2 to 50.7°C for solar irradiation of 450 W/m², and 29.1 to 53.1°C for the solar irradiation 500 W/m² respectively.

The streamlines plot of the PVT system with a cooling system is shown in figure 3.2 for solar irradiation levels ranging from 250 W/m² to 500 W/m² at a fixed mass flow rate of 0.054 Kg/s and inflow temperature of 30°C. Surface temperatures range from 26.5 to 40.7°C for solar irradiation of 250 W/m², from 25.9 to 42.9°C for solar irradiation of 300 W/m², from 25.2 to 45.1°C for solar irradiation of 350 W/m², from 24.5 to 47.2°C for solar irradiation of 400 W/m², from 23.9 to 49.4°C for solar irradiation of 450 W/m², and from 23.2 to 51.6°C for solar irradiation of 500 W/m², respectively.

The simplified plot also has a color expression. The fluid's temperature can be determined using the temperature bar (°C). The fluid's average temperature at the exit port increases as irradiation values climb. This is so that more heat can be produced by the solar cell as a result of higher solar irradiation, which also raises the surface temperature of the PV module.

3.3 Effect of Mass Flow Rate

The surface temperature plot for the PVT system with 450 W/m² illumination and 30°C inflow temperature is shown in figure 3.3 as a function of the inlet fluid (air) mass flow rate. The mass flow rates, which are 0.0063, 0.0109, 0.023, 0.0323, 0.047, and 0.23 m/s, respectively, are 0.015, 0.025, 0.054, 0.075, 0.109, and 0.535 kg/s. PVT surface temperatures range from 28.9 to 71°C for mass flow rate of 0.015 kg/s, 28.9 to 66.6°C for mass flow rate of 0.025 kg/s, 29.2 to 50.7 kg/s for mass flow rate of 0.054 kg/s, 29.2 to 44.7 kg/s for mass flow rate of 0.075 kg/s, 29.3 to 41.5 kg/s for mass flow rate of 0.109 kg/s, and 29.6 to 33.3 kg/s for mass flow rate of 0.535 kg/s respectively. when seen in this diagram, when the mass flow rate increases, thermal current activity increases via the heat exchanger surface and into the fluid flow domain. The hue of the surface close to the PVT system's outflow port initially darkens as the mass flow rate rises but gradually becomes lighter. As the mass flow rate is increased from 0.015 to 0.535 kg/s, the temperature distribution changes, increasing overall heat transfer. It is found that the maximum temperature of the PVT material gradually falls as the mass flow rate of the incoming fluid rises. At the lowest flow rate (0.015 kg/s), the temperature rises to its maximum; at the

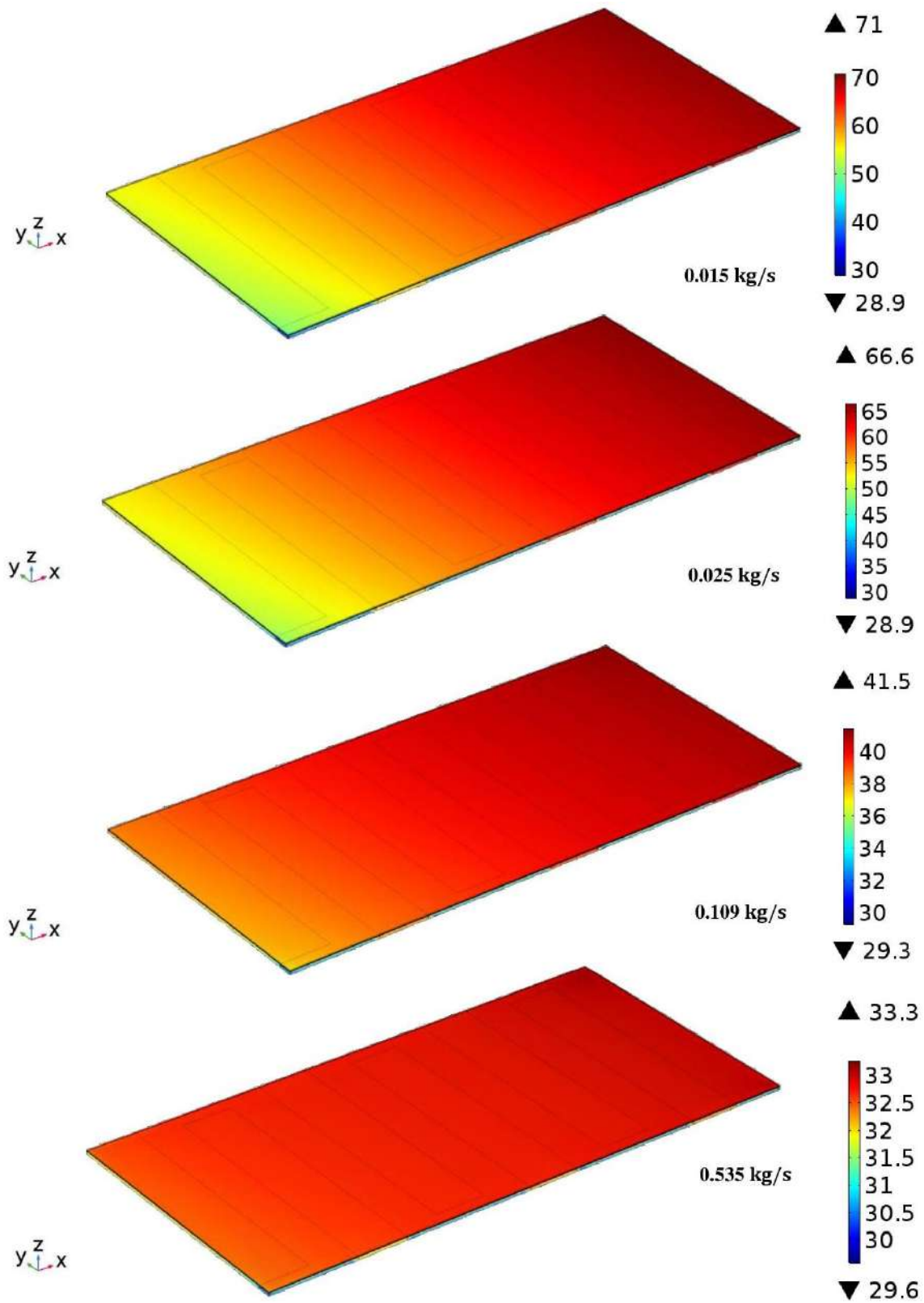


Figure 3.3: Surface temperature of PVT system for the variation of mass flow rate from 0.015 to 0.535 Kg/s at irradiation level of 450 W/m², and inflow temperature of 30°C

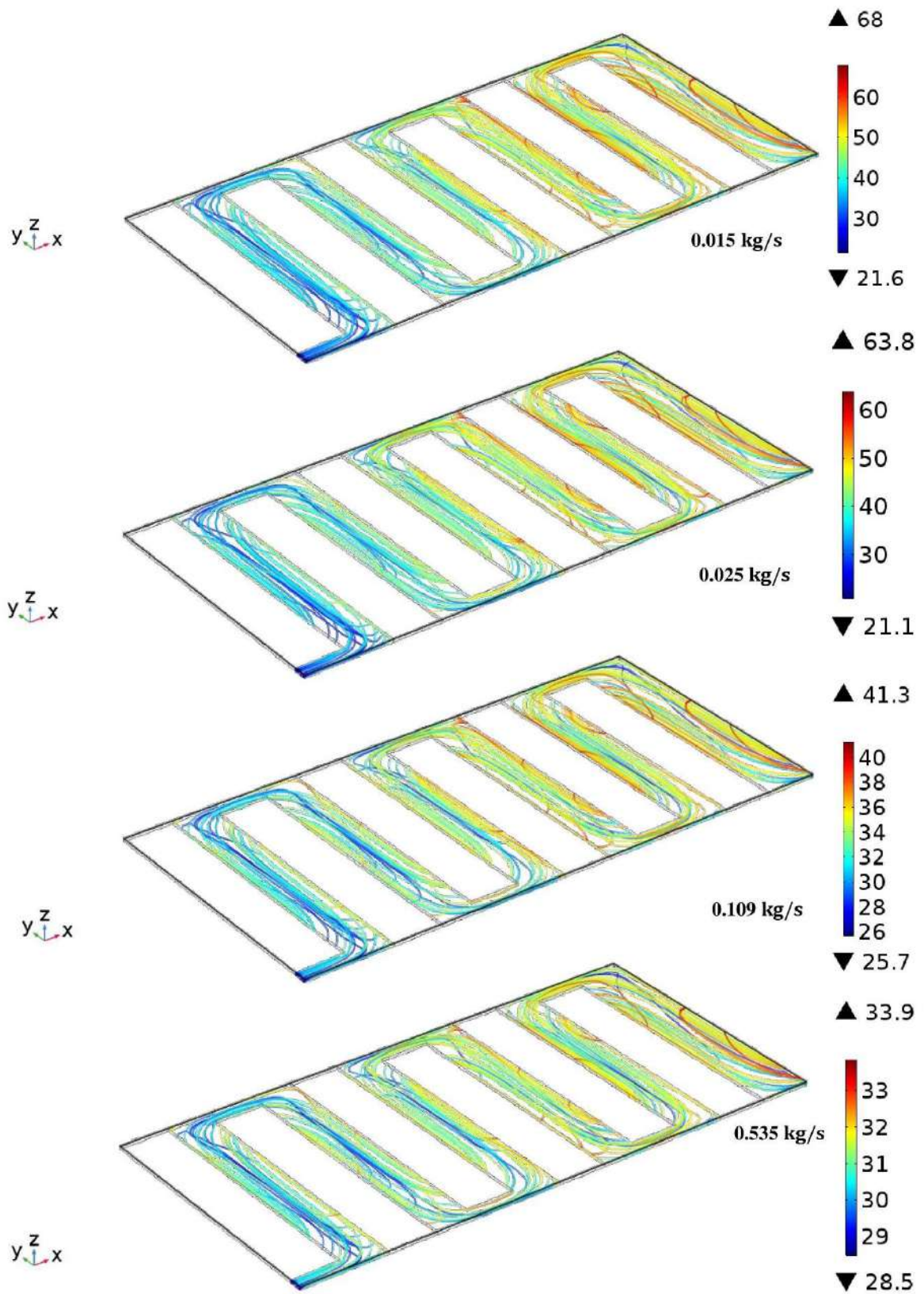


Figure 3.4: Streamlines plot of PVT system for the variation of mass flow rate from 0.015 to 0.535 Kg/s at irradiation level of 450 W/m², and inflow temperature of 30°C

highest flow rate (0.535 kg/s), it decreases to its minimum. For fluid flow characteristics with dominant behavior, this is the case.

Thus, from the top glass surface to the outlet exit, conductive and convective heat transfer processes take place through the heat exchanger of the PVT system. The PVT system's simplified plot with the cooling system at various mass flow rates is shown in figure 3.4. In this simulation, solar irradiation is adjusted at 450 W/m^2 . When the mass flow rate is decreased, the temperature of the fluid at the exit port increases. The temperature of the fluid lowers as the mass flow rate rises.

This is important because a fluid that is flowing quickly cannot take in more heat from the heat exchanger in the PVT system. This graphic shows the fluid flow distribution from the entrance port to the outlet port. The range of fluid temperature is discovered from 21.6 to 68°C for mass flow rate of 0.015 kg/s , from 21.1 to 63.8°C for mass flow rate of 0.025 kg/s , from 23.9 to 49.4°C for mass flow rate of 0.054 kg/s , from 24.8 to 44.4°C for mass flow rate of 0.075 kg/s , from 25.7 to 41.3°C for mass flow rate of 0.109 kg/s , from 28.5 to 33.9°C for mass flow rate of 0.535 kg/s respectively.

3.4 Effect of Inflow Temperature

The surface temperature curve in figure 3.5 shows the impact of inflow temperature on a PVT system. Temperature readings for the inflow are made at 10 , 20 , 25 , 30 , 35 , and 40°C . This temperature range encompasses Bangladesh's whole six-season temperature range. In this case, the mass flow rate is set to 0.054 kg/s , while the sun's irradiation is set at 450 W/m^2 . The surface temperature of the PV module lifts from 4.98 to 31°C at 10°C inflow temperature. Similarly, it lifts from 15 to 40.9°C at 20°C inflow temperature, from 20 to 45.9°C at 25°C inflow temperature, from 29.2 to 50.7°C at 30°C inflow temperature, from 30 to 55.9°C at 35°C inflow temperature, and from 35 to 60.9°C at 40°C inflow temperature. Figure 3.6 depicts the streamlines plot showing the effect of input temperature on the PVT system. The fluid temperature of the PV module lifts from 9.52 to 30°C at 10°C inflow temperature. Similarly, it lifts from 19.5 to 40°C at 20°C inflow temperature, from 24.5 to 45°C at 25°C inflow temperature, from 23.9 to 49.4°C at 30°C inflow temperature, from 34.5 to 55°C at 35°C inflow temperature, and from 39.5 to 59.9°C at 40°C inflow temperature.

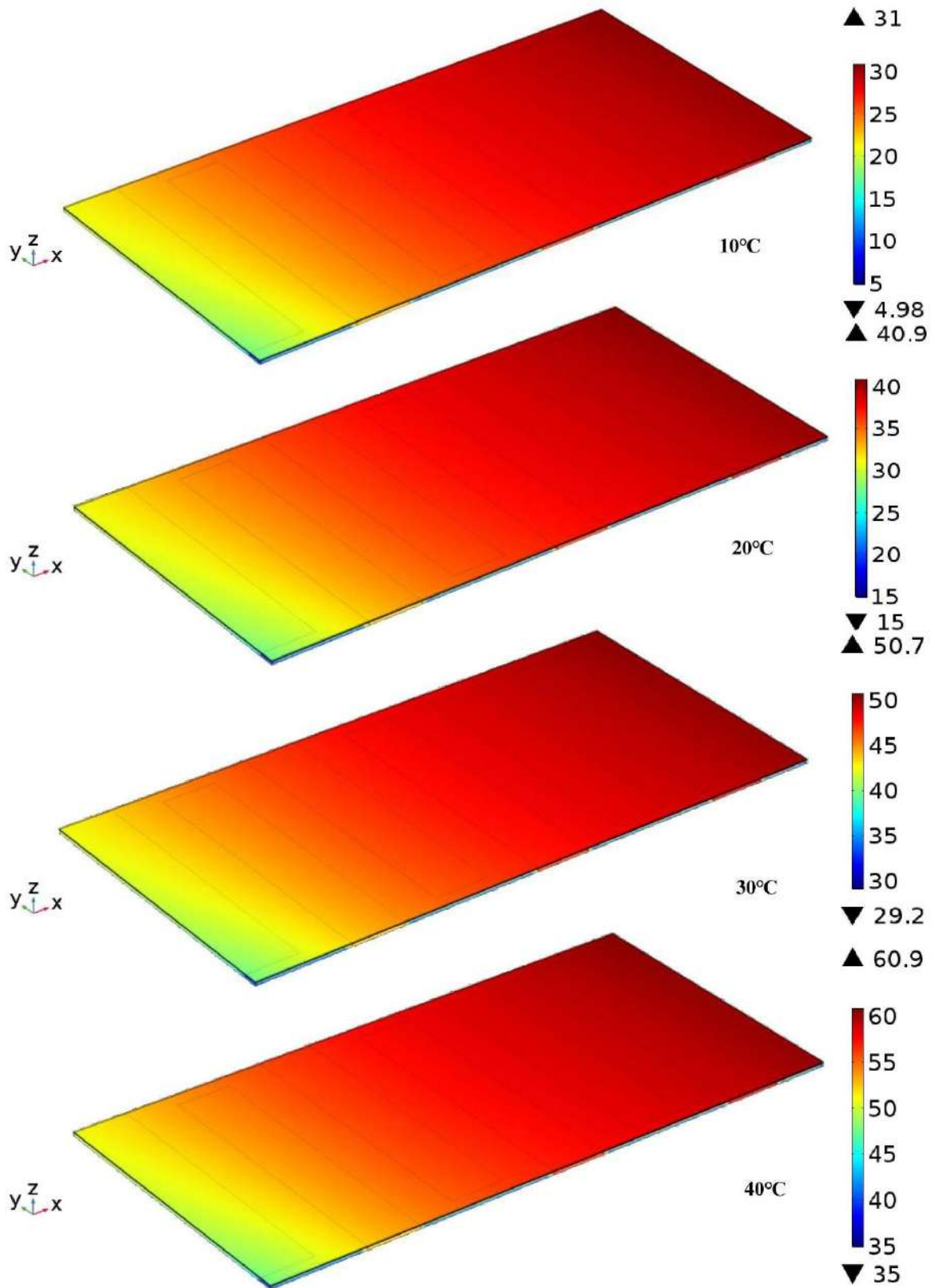


Figure 3.5: Surface temperature of PVT system for the variation of inflow temperature from 10°C to 40°C at 0.054 Kg/s, and irradiation level at 450 W/m²

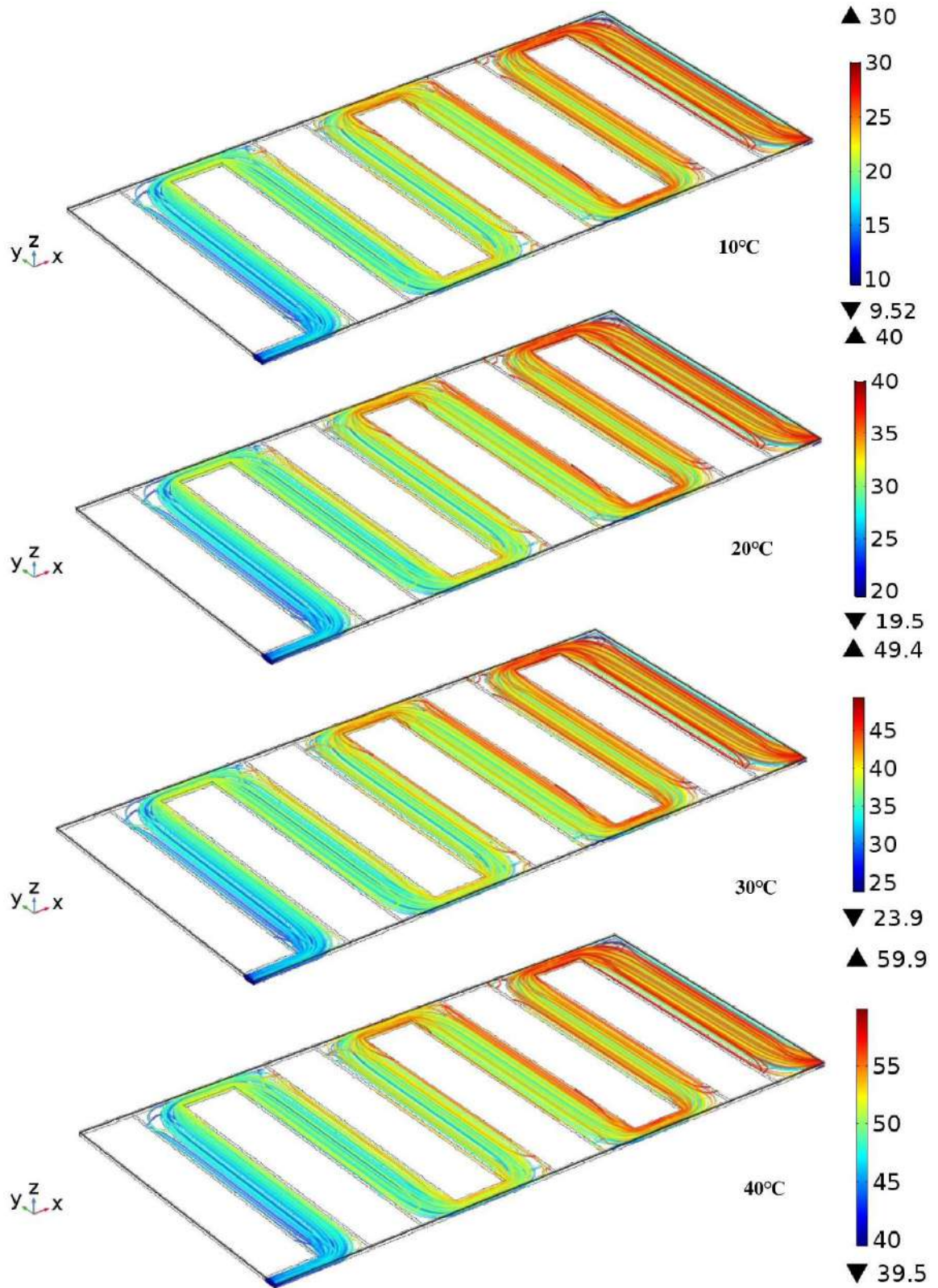


Figure 3.6: Streamlines plot of PVT system for the variation of inflow temperature from 10°C to 40°C at 0.054 Kg/s, and irradiation level at 450 W/m²

3.5 Cell Temperature

Figure 3.7(a)–(c) depicts the solar cell temperature for the effects of solar irradiation, mass flow rate, and inflow temperature, respectively. It is clear from this work that the average solar cell temperature, the heat exchanger surface temperature, the ambient temperature, and incident irradiance all have a significant relationship.

Figure 3.7(a) indicates that, for the variation of irradiation from 250 W/m^2 to 500 W/m^2 , the cell temperature rises by 8.49°C in the PVT system with a cooling system of 0.054 kg/s mass flow rate and an inflow temperature of 30°C . The current results display that each 50 W/m^2 rise in irradiation hikes the cell temperature by around 1.698°C . This study's objective is to use an appropriate cooling mechanism to maintain the cell temperature within a specific range so that the PV material doesn't deteriorate.

Figure 3.7(b) represents that, in the irradiation level 450 W/m^2 , input fluid temperature 30°C , the cell average temperature air declines as the inflow fluid mass flow rate rises from 0.015 to 0.535 kg/s . When the incoming fluid mass flow rate is increased, convection removes more heat from the module. The average cell temperature has decreased as a result. As the mass flow rate rises, the cell means temperature rapidly decreases, as depicted in this graph. The mass flow rate is initially 0.015 kg/s , and the solar cell temperature is 56°C . The temperature of the cell gradually falls up to a mass flow rate of 0.535 kg/s . Moreover, the mass flow rate rises to 0.535 kg/s , the temperature falls to 37°C , however, the pumping capacity is unchanged. The temperature of the solar cell falls by 3.8°C for every 0.097 kg/s rise in incoming fluid mass flow rate.

Figure 3.7(c) indicates that as the input fluid temperature ($10\text{--}40^\circ\text{C}$) increases, the convective heat transfer from the PVT system to the surrounding air decreases. As a result, convection increases the average cell temperature by removing less heat from the PVT system to around 26.028 , 36.011 , 41.002 , 45.13 , 50.982 , and 55.972°C for inflow temperatures of 10 , 20 , 25 , 30 , 35 and 40°C , respectively. For each 5°C rise in inflow temperature, solar cell temperature rised by about 4.99°C .

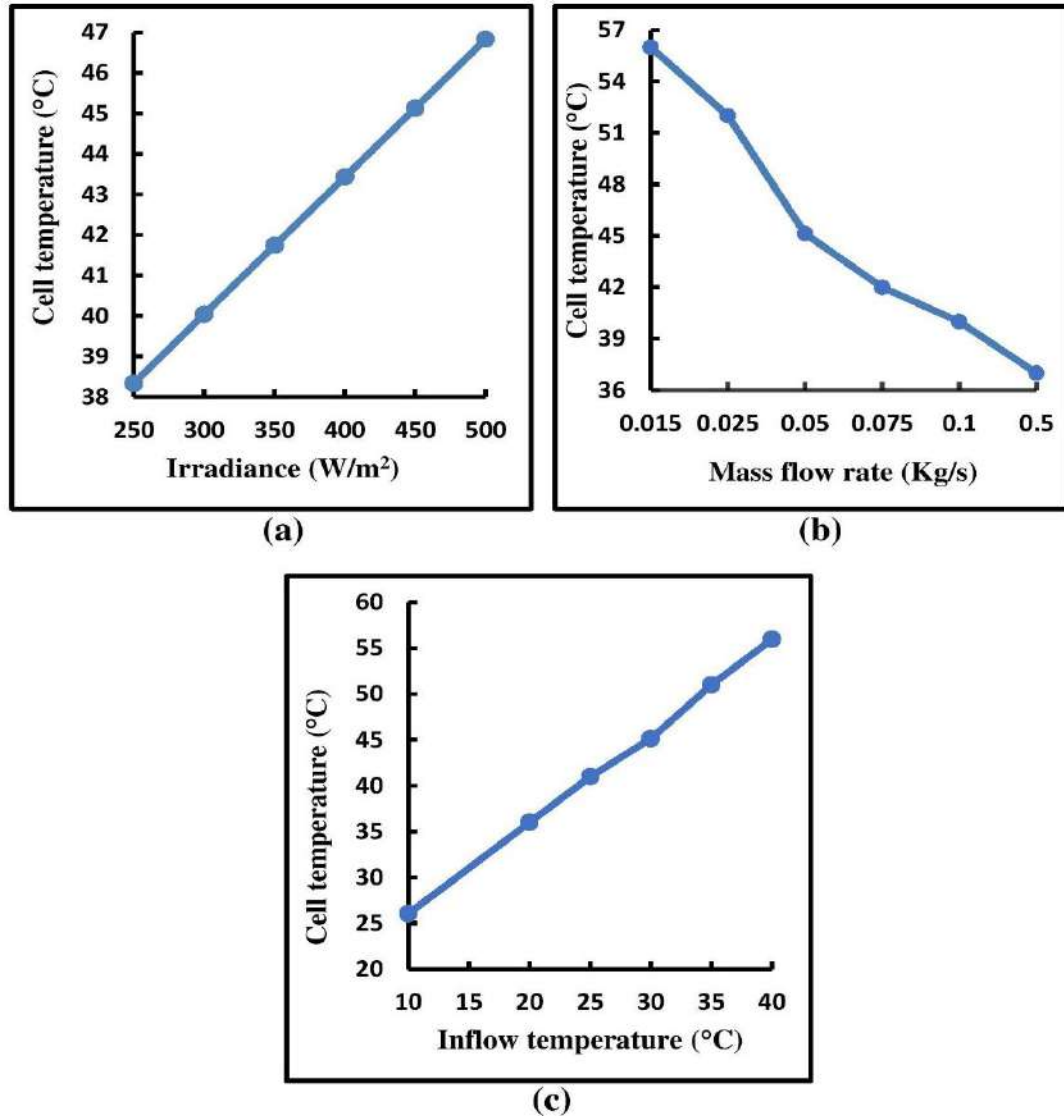


Figure 3.7: Solar cell temperature for the effect of (a) irradiance, (b) mass flow rate, (c) inflow temperature

3.6 Electrical Power

Figure 3.8(a)-(c) indicates the total amount of electrical power produced for various irradiation (250 - 500 W/m²), mass flow rate (0.015 - 0.535 kg/s), and inflow temperature (10 - 40°C).

Figure 3.8(a) indicates that the starting irradiation level is 250 W/m² and the output power is 48.73 W, while the electrical power is 93.5 W at a 500 W/m² irradiation level. The electrical power of a PVT system with a cooling system at a mass flow rate of 0.054 kg/s and an inflow temperature of 30°C rises by 8.954 W for every 50 W/m² hikes in irradiation level. This is due

to the PV module's size, packing factor, reference temperature, operating conditions, incorrect cooling system installation, and material quality.

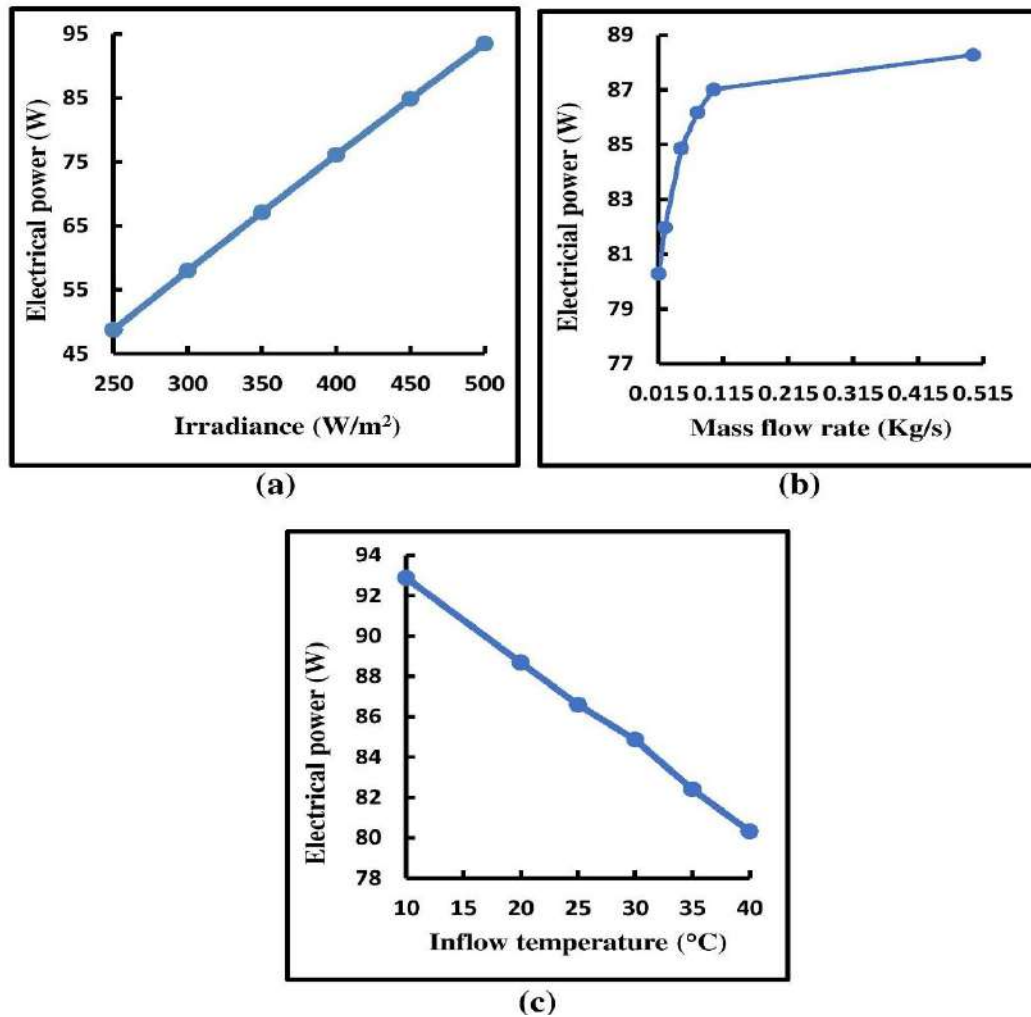


Figure 3.8: Electrical power for the effect of (a) irradiance, (b) mass flow rate, (c) inflow temperature

Figure 3.8(b) represents that, the initial mass flow rate is 0.015 kg/s and the electrical power is 80.29 W at a fixed irradiation level of $450 W/m^2$ under various fluid mass flow rates. The output power hikes to 88.27 W at a mass flow rate of 0.535 kg/s. With a rise in fluid mass flow rate of about 0.52 kg/s, the output power rises by 7.98 W. For every 0.097 kg/s rise in fluid mass flow rate, the output power hike by 1.596 W under cooling conditions.

Figure 3.8(c) indicates the change of electrical power as a function of inflow temperature. For rising inflow temperature values from 10 to $40^{\circ}C$, the electrical power against inflow

temperature is 92.88, 88.69, 86.59, 84.86, 82.4, and 80.31 W, respectively. For each 5°C rise in inflow temperature, electrical power declines by about 2.095 W. As the inflow temperature hikes, the convective heat transfer phenomenon declines. As a result, the PVT system's electrical power generation is trending downward.

3.7 Electrical Efficiency

Figure 3.9(a)-(c) indicates the percentage of electrical efficiency of the PVT module as a function of solar irradiance, mass flow rate, and inflow temperature ranging from 250 to 500 W/m², 0.015 kg/s to 0.535 kg/s, and 10 to 40°C.

The electrical efficiency of the modules declines as solar irradiation rises, as shown in figure 3.9(a). At the highest mass flow rate of 0.054 kg/s, the electrical efficiency of the PVT module falls from 14.1 to 13.53% as the irradiation level hikes. As a result, for each 50 W/m² rise in irradiation, electrical efficiency declines by about 0.114%.

Figure 3.9(b) constitutes that, the maximum electrical efficiency is around 14.19%. For every 0.097 kg/s rise in mass flow rate, electrical efficiency rises by about 0.256%. The average temperature of the cell is diminished as the incoming mass flow rate of air rises. As a result, PVT voltage substantially rises while PVT current somewhat decreases, boosting electrical efficiency and output power.

The electrical efficiency with the variation of inflow temperature is showed in figure 3.9(c). From the figure, for inflow temperatures of 10, 20, 25, 30, 35, and 40°C, respectively, the electrical efficiency of PVT systems declines by 14.93, 14.26, 13.92, 13.64, 13.25, and 12.91%. This study demonstrates that electrical efficiency decreases by around 0.34% for every 5°C increase in inflow temperature. Thus, the current new PVT system works well to achieve greater efficiency.

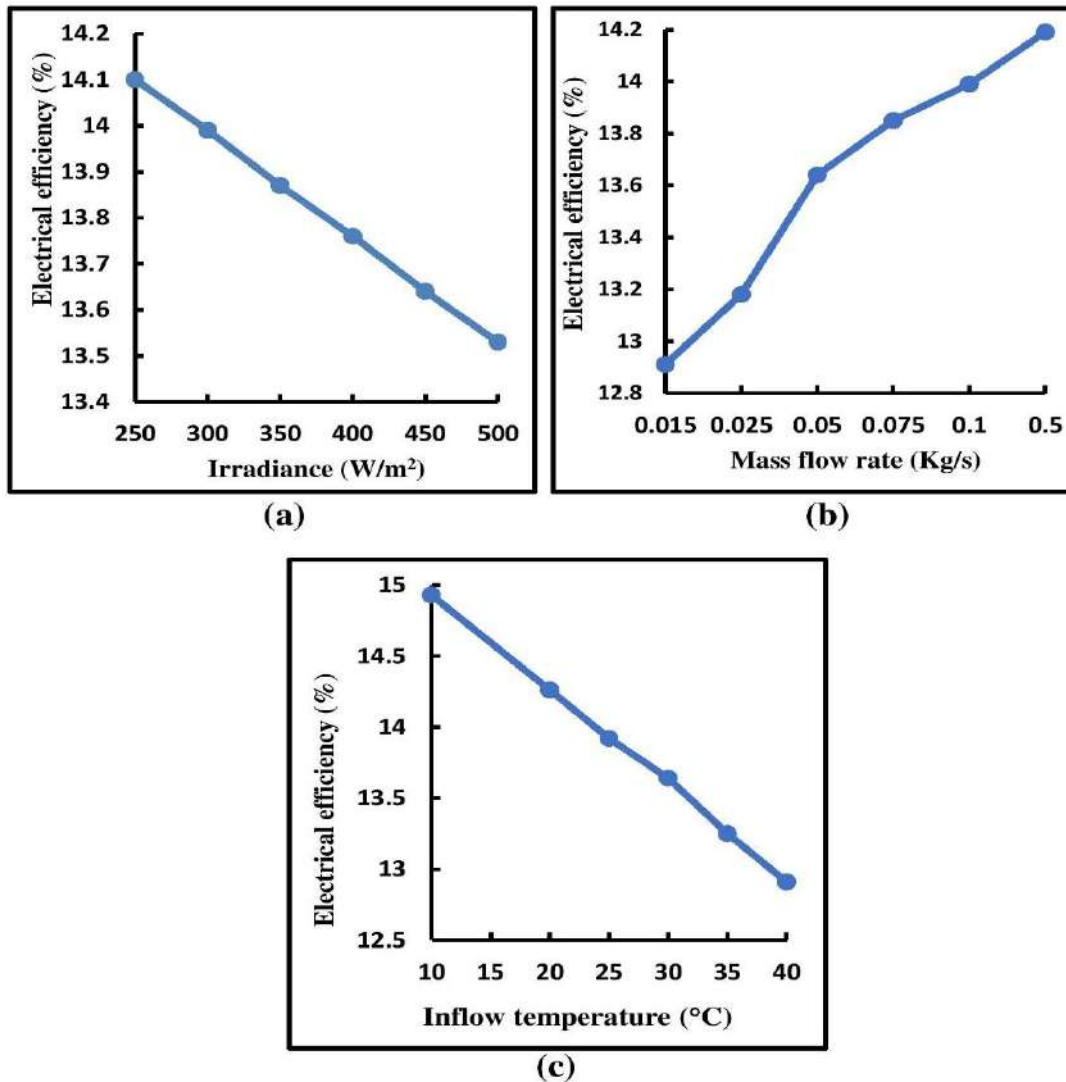


Figure 3.9: Electrical efficiency for the effect of (a) irradiance, (b) mass flow rate, (c) inflow temperature

3.8 Outlet Fluid Temperature

The change of output fluid temperature for the effect of solar irradiation (250 - 500 W/m²), (0.015 - 0.535 kg/s), and inflow temperature (10 - 40°C) is represented in figure 3.10 (a)-(c).

As irradiation levels hike, the temperature of the fluid output hikes. When the irradiation intensity is 250 W/m², the output fluid temperature is approximately 35.365°C at a fixed mass flow rate of 0.054 kg/s and an inflow fluid temperature of 30°C as shown in figure 3.10(a). The fluid outlet means temperature rises to 36.42°C at 300 W/m², 37.45°C at 350 W/m², 38.48°C at

400 W/m², 39.515°C at 450 W/m², and 40.52°C at the highest irradiation of 500 W/m². Moreover, outlet fluid temperature rises by approximately 1.03°C for each addition of 50 W/m² solar irradiation.

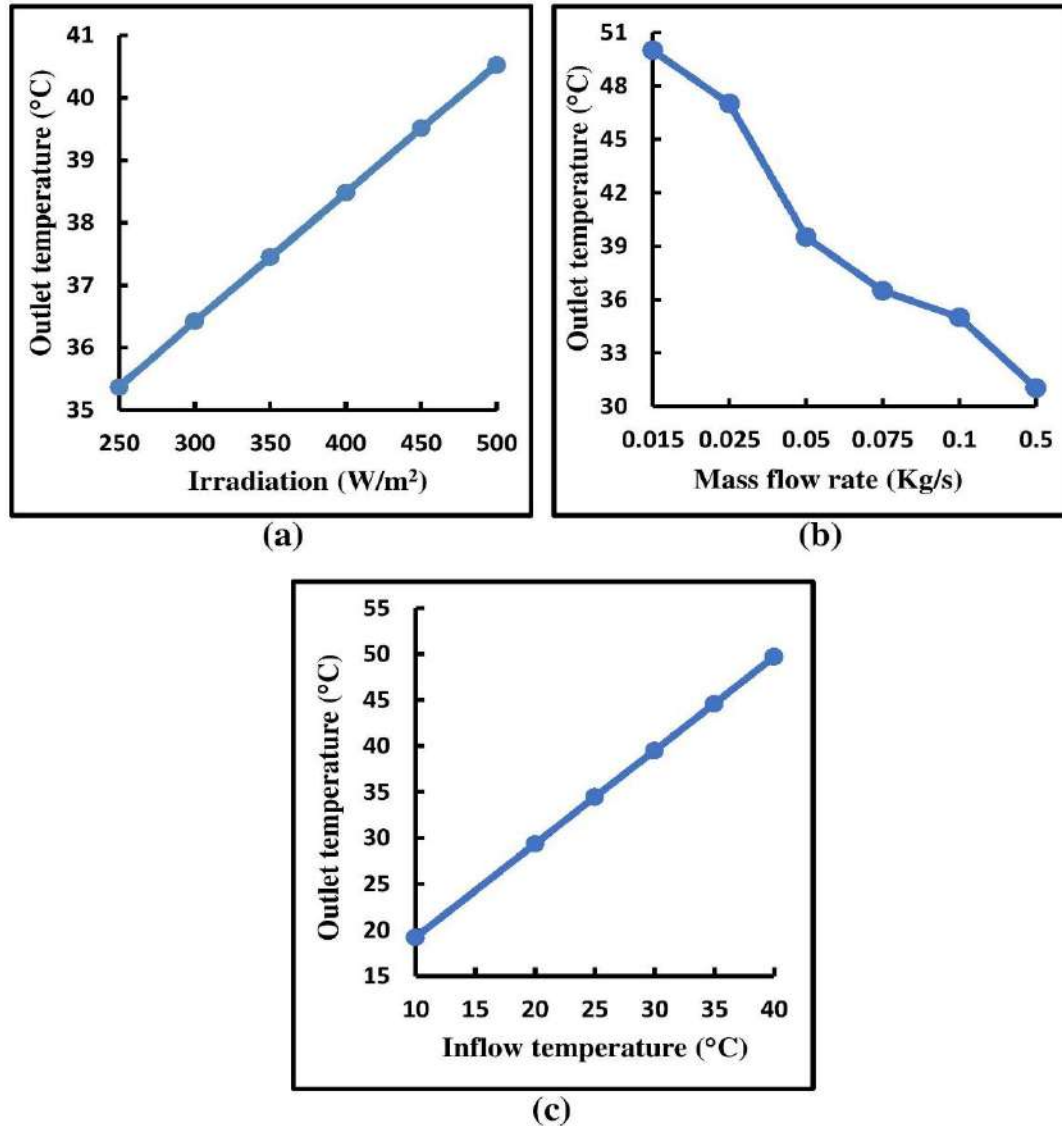


Figure 3.10: Outlet fluid temperature for the effect of (a) irradiance, (b) mass flow rate, (c) inflow temperature

Figure 3.10(b) indicates that, at a given input temperature of 30°C and irradiation of 450 W/m², the air outlet temperature falls as the inflow mass flow rate rises. The declining trend may also be caused by the increased convection heat transfer rate with increasing velocity. There is less time for thermal accumulation as the mass flow velocity increases, which lowers the air outlet temperature and increases the rate of heat evacuation. When the mass flow rate is 0.015 kg/s,

the output fluid temperature is approximately 50°C and at the highest mass flow rate 0.535 kg/s, the output fluid temperature is around 31.02°C. Moreover, outlet fluid temperature declines by approximately 3.796°C for each addition of 0.097 kg/s mass flow rate. The mass flow rate gradually decreases till it reaches 0.535 kg/s as it increases. The mass flow rate of 0.535 kg/s is therefore the one that will increase the PVT system's efficiency the most.

The outlet temperature with the variation of inflow temperature at a fixed irradiation level of 450 W/m² is displayed in figure 3.10(c). From the figure, for inflow temperatures of 10, 20, 25, 30, 35, and 40°C, respectively, the outlet temperature of the PVT system is 19.2, 29.35, 34.45, 39.515, 44.6, and 49.7°C. The temperature at the outflow increased by around 5.08°C for every 5°C rise at the entrance.

3.9 Thermal Energy

The extracted thermal energy from the system is shown in figure 3.11(a)–(c) as a function of solar irradiation, mass flow rate, and inflow temperature.

The extracted thermal power in the PVT system at 250 W/m² irradiation is 270 W. For an irradiation level of 500 W/m² and a fixed mass flow rate of 0.054 kg/s, this energy becomes 530 W. This is caused by conductive heat flow from the heat exchanger's top glass surface as well as convective heat flow from the heat exchanger to the moving fluid. As a result, there is more radiation possible due to the growing temperature difference between the fluids at the output and inlet. Figure 3.11(a) displays that for every 50 W/m² rise in irradiation, the system removes 52 W thermal energy.

When the mass flow rate is 0.015 kg/s, the total quantity of thermal energy gathered from the system is 302 W. The amount of thermal energy is found to be 514 W at the greatest mass flow rate of 0.535 kg/s as shown in figure 3.11(b). However, the rate at which the temperature of the outlet fluid declines is significantly impacted by increasing the cooling fluid mass flow rate (0.015–0.535 kg/s). The exit fluid's temperature gradually drops when the mass flow rate is raised to 0.535 kg/s. As a result, the system's ability to extract thermal energy steadily gets better as the mass flow rate of the cooling fluid approaches 0.535 kg/s. For every 0.097 kg/s increase in mass flow rate, 42.4 W more thermal energy may be extracted.

The thermal energy with the variation of inflow temperature at a fixed irradiation level of 450 W/m² is displayed in figure 3.11(c). From the figure, it can be seen that for inflow temperatures of 10, 20, 25, 30, 35, and 40°C, respectively, the thermal energy of PVT modules is 463 W, 471 W, 476 W, 479 W, 483 W, and 488 W. It is obvious to see that the amount of thermal energy increased by around 4.12 W for every 5°C rise in the inflow temperature.

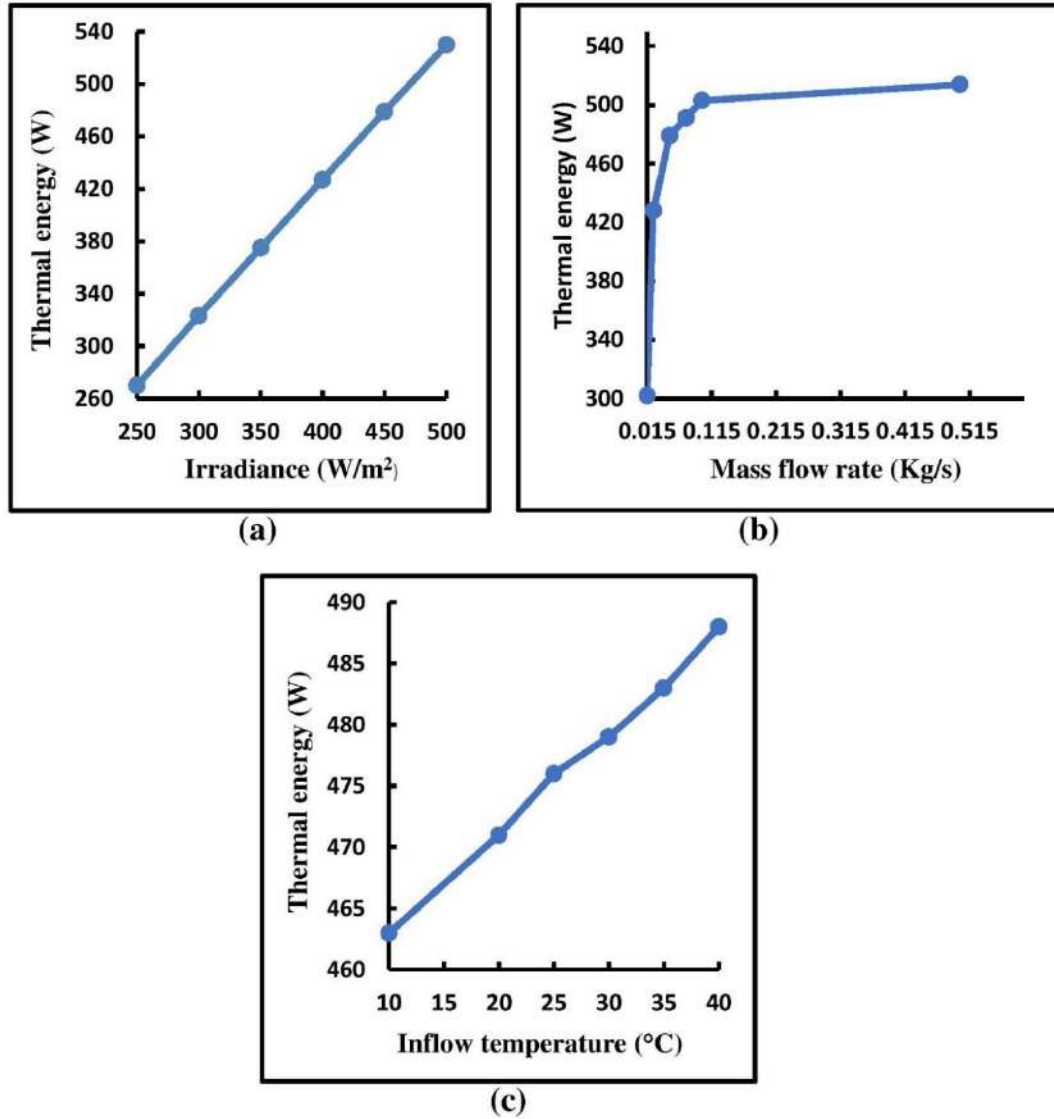


Figure 3.11: Thermal energy for the effect of (a) irradiance, (b) mass flow rate, (c) inflow temperature

3.10 Thermal Efficiency

As a function of solar irradiation, mass flow rate, and inflow temperature, figure 3.12(a)-(c) shows the thermal efficiency of the system.

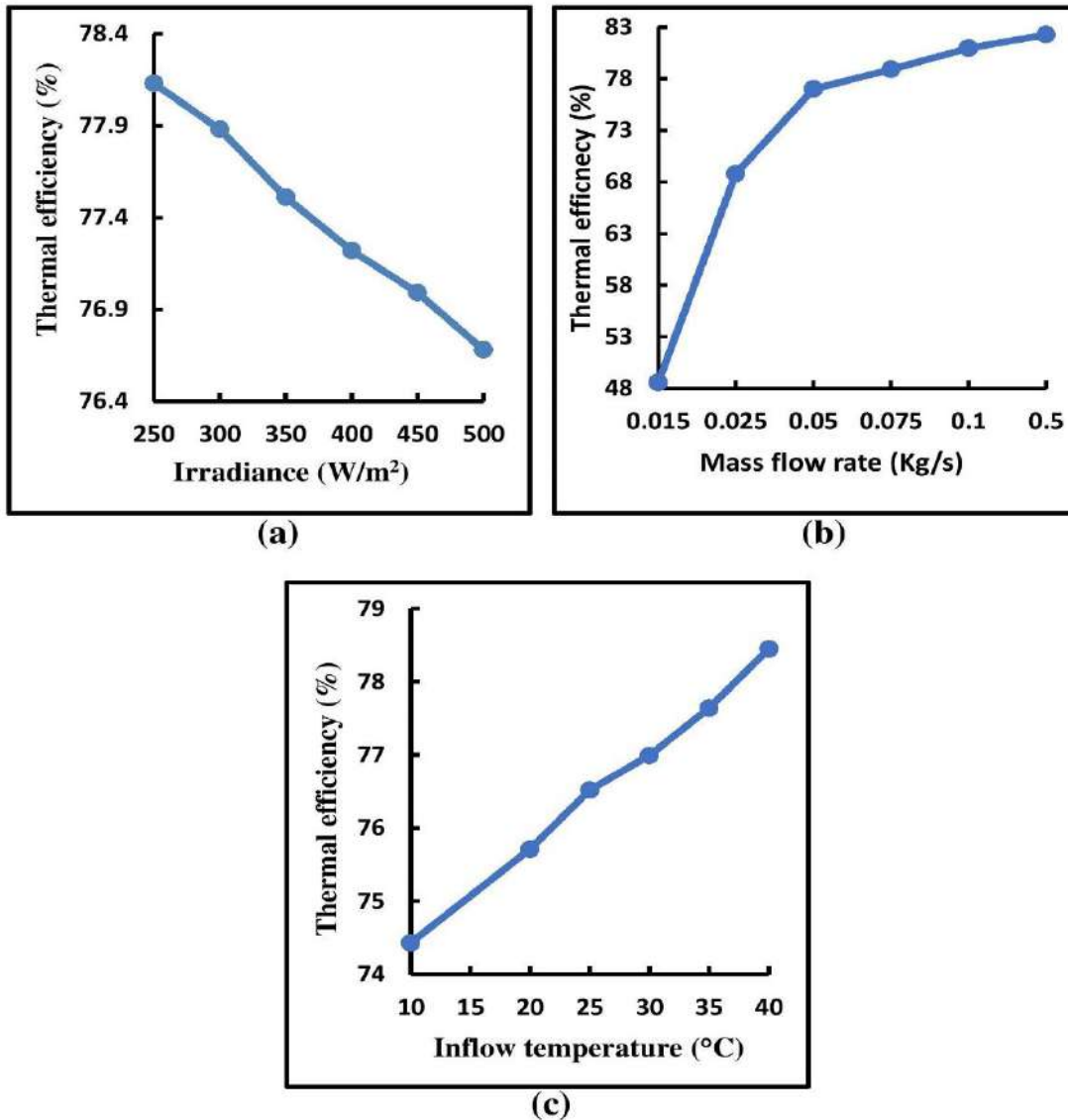


Figure 3.12: Thermal efficiency for the effect of (a) irradiance, (b) mass flow rate, (c) inflow temperature

It may be observed in figure 3.12(a) that, when the solar irradiation level rises 250 to 500 W/m^2 , the thermal efficiency declines at a given mass flow rate of 0.054 kg/s. With a change in irradiance, thermal efficiency falls from 78.13% to 76.68%. For every 50 W/m^2 rise in solar irradiation, there is a 0.29% decline in thermal efficiency.

By raising the mass flow rate from 0.015 to 0.535 kg/s, the convective heat transfer coefficient of air is enhanced. As a result, thermal efficiency is improved since more heat is transferred at faster rates when there is a given temperature difference. In terms of mass flow rate, the thermal efficiency increases for this numerical simulation from 48.57% to 82.26%. It is challenging to

increase the efficiency rate since the fluid mass flow rate ranges from 0.015 to 0.535 kg/s. However, there is only a significant improvement in thermal efficiency for a mass flow rate of 0.025 kg/s. The temperature of solar cells actually steadily decreases as cooling fluid mass flow rate rises (up to 0.535 kg/s). The temperature of the solar cell decreases slightly when the mass increase the efficiency rate since the fluid mass flow rate ranges from 0.015 to 0.535 kg/s. However, there is only a significant improvement in thermal efficiency for a mass flow rate of 0.025 kg/s. The temperature of solar cells actually steadily decreases as cooling fluid mass flow rate rises (up to 0.535 kg/s). The temperature of the solar cell decreases slightly when the mass flow rate is higher than 0.054 kg/s. Figure 3.12(b) shows that the thermal efficiency increases by approximately 6.738% when the mass flow rate of the incoming air is raised by 0.097 kg/s. Figure 3.12(c) shows the thermal efficiency as a function of inflow temperature at a fixed irradiation level of 450 W/m². The thermal efficiency of PVT systems is 74.43, 75.71, 76.52, 76.99, 77.64, and 78.45% respectively, for inflow temperatures of 10, 20, 25, 30, 35, and 40°C, respectively. It is simple to understand how an increase of 5°C in the input temperature increased thermal efficiency by about 0.67%.

3.11 Overall Efficiency

Figure 3.13(a)-(c) displays the PVT system's overall efficiency graph for the influences of solar irradiation, mass flow rate, and inflow temperature.

With rising irradiation values from 250 to 500 W/m² at 0.054 kg/s mass flow rate and 30°C inflow temperature, it reduces from 92.23% to 90.21%. Figure 3.13(a) shows that the overall efficiency decreases by 0.404% for every 50 W/m² increase in irradiation level.

The total efficiency increases as the electrical and thermal efficiencies increase with the inflow mass flow rate, as shown in figure 3.13(b). As a result, the overall efficiency is 61.48% at a decreased mass flow rate of 0.015 kg/s. The mass flow rate increases significantly by up to 96.45% when it is raised to 0.535 kg/s. Overall efficiency rises by 6.994% for each 0.097 kg/s increase in mass flow rate.

Figure 3.13(c) indicates the total efficiency as a function of inflow temperature at a given irradiation level of 450 W/m². The overall efficiency of PVT modules is 89.36, 89.97, 90.44, 90.63, 90.89, and 91.36% respectively, for inflow temperatures of 10, 20, 25, 30, 35, and 40°C.

It is simple to understand how an increase in input temperature of 5°C increases overall efficiency by about 0.33 percent. The temperature of the fluid entering a PVT system is important for increasing overall effectiveness.

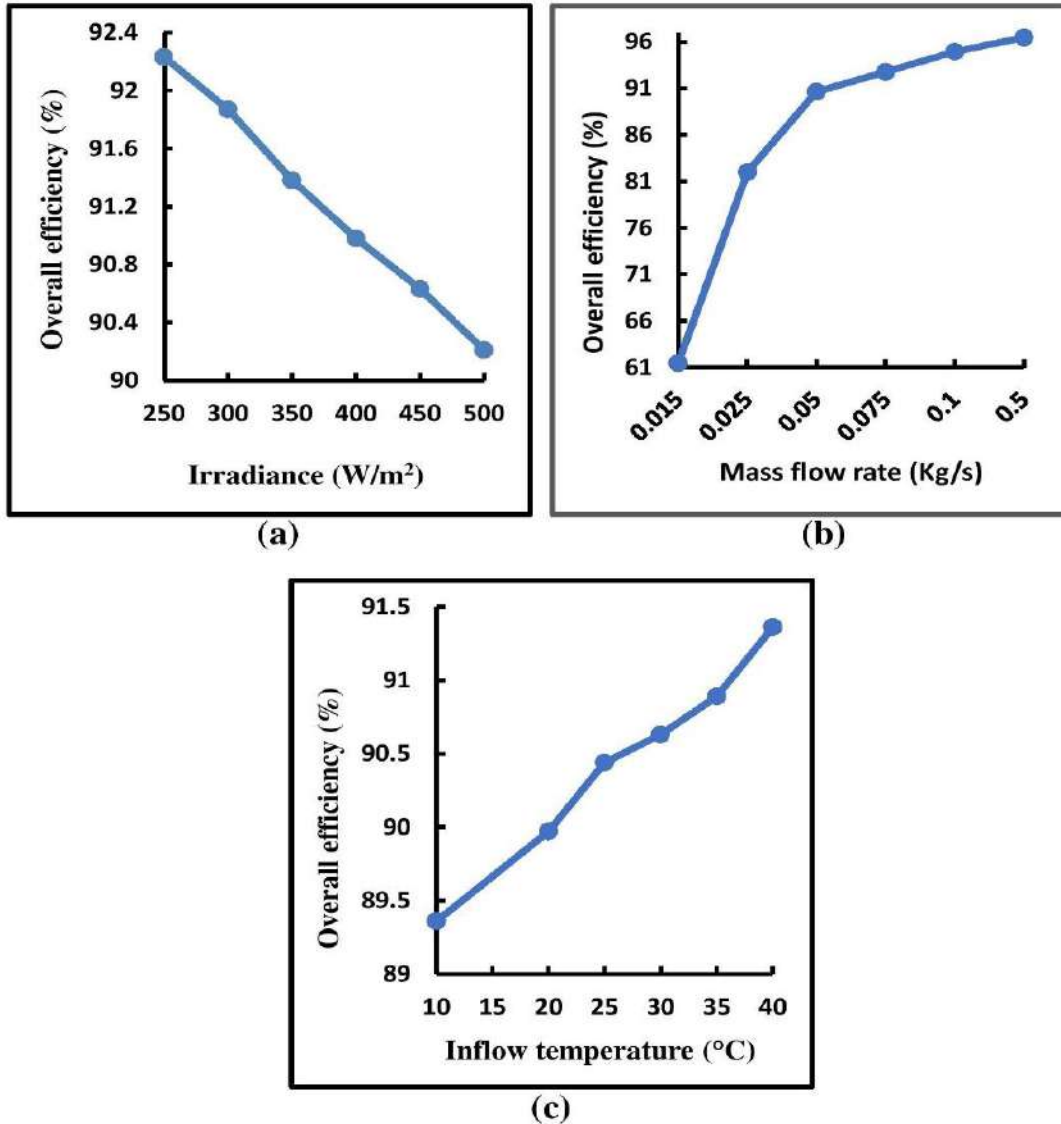


Figure 3.13: Overall efficiency for the effect of (a) irradiance, (b) mass flow rate, (c) inflow temperature

3.12 Comparison

The currently available numerical finding has been contrasted with earlier research by Zohora et al. [22], Rahman et al. [29], Chandrasekar et al. [32], and Bahaidarah et al. [33]. For 100 W/m^2 , overall efficiency dropped by 0.83% as studied by Zohora et al. [22], and output power increased by 3.14 W as examined by Rahman et al. [29] where water is the working fluid for both cases. Under outdoor operating conditions, Chandrasekar et al. [32] found that decreased the solar cell temperature by 20°C while increasing the output power by 6.5 W and electrical efficiency by 1.4% where a cooling system is included composed of water, Al_2O_3 /water nanofluid, and CuO /water nanofluid in combination with cotton wick structures. A rear surface water-cooling device by Bahaidarah et al. [33] also reduced solar cell temperature by 20% while raising electrical efficiency by about 9%. Compared to Zohora et al. [22], Chandrasekar et al. [32], and Bahaidarah et al. [33], the water-cooling system used in the study by Rahman et al. [29] performs better. The comparison of performance enhancements by cooling systems used in various research is shown in table 3.2. In this research, we have used air as the working fluid for the proposed PVT system. For the current numerical result and previous experimental results, a strong pattern of similarity is seen.

Table 3.2: PVT cell temperature comparison with a few research

Authors, year, time, and location	Irradiation (W/m ²)		Operating temperature (°C)		Maximum ambient temperature (°C)	Cell temperature increment per 50 W/m ² irradiation
	At starting period	At peak period	At starting period	At peak period		
Zohora et. al. [22], August 2022, Bangladesh, Latitude 23.7266° N, longitude 90.3927° E	200	500	27	40.4	27	1.085
Rahman et al. [29], March 2015, University of Malaya, Solar Park at Level 3, Wisma R&D, Malaysia, Latitude 3.1209° N, longitude 101.6538° E	312	995	31	50	35	1.36
Chandrasekar et al. [32], April, 2013, Anna University, BIT campus, Tiruchirappalli, India. Latitude 10°39'N, longitude 78°44'E	600	1300	40	50	37	0.7
Bahaidarah et al. [33], February, 2012, KFUPM, Dhahran, Saudi Arabia. Latitude 26°18'N, longitude 50°08'E	240	979	21	35	21	0.95
In the current numerical investigation	250	500	30	52.4	30	1.6

CONCLUSIONS AND FUTURE RESEARCH

The conclusions of this thesis are of utmost significance since they summarize the results and findings of the in-depth investigation done. These conclusions give a thorough review of the major findings and emphasize the importance of the study in relation to the study's research questions or aims. They are a useful tool for both researchers and practitioners, providing information that can be used to make decisions and encourage more development in the subject. Basically, the findings in this thesis add to the existing information base and inspire more research and real-world applications.

4.1 Conclusions

The findings show that the performance of PVT is significantly influenced by solar irradiation, cooling fluid mass flow rate, and inflow temperature. As the irradiation and cooling mass fluid flow rates climb, the PVT system's capacity to produce electrical power and convert thermal energy increases. This module's inflow temperature has been numerically observed and plays a significant role. This section contains particular findings and outlines for additional research that have been made in light of the results of the numerical investigation are shown in table 4.1.

Table 4.1: Conclusions from the present research

Solar irradiation	For the increases of every 50 W/m ² solar irradiation, the cell and outlet temperature, electrical power and thermal energy increase by approximately 1.698°C and 1.03°C, 8.954 W and 52 W respectively
	The electrical, thermal, and overall efficiencies decrease by about 0.114%, 0.29%, and 0.404% for each 50 W/m ² increase of irradiation
Mass flow rate	The cell temperature and outlet fluid temperature decrease by approximately 3.8°C and 3.796°C respectively; electrical power and thermal energy increase by about 1.596 W and 42.4 W respectively for the increases of every 0.097 kg/s fluid mass flow rate
	For the increment of every 0.097 kg/s fluid mass flow rate, the electrical, thermal, and overall efficiencies increase by about 0.256%, 6.738%, and 6.994%
Inflow temperature	For every 5°C increments of inflow temperature solar cell temperature and outlet temperature increase 4.99°C and 5.08°C, electrical power decreases to 2.095 W and thermal energy increase to 4.17 W
	For the increment of every 5°C increments of inflow temperature, the electrical efficiency decreases by about 0.34%, thermal, and overall efficiencies increase by about 0.67%, and 0.33%

4.2 Future Research

The purpose of this study was to determine how the power generation of a PVT system in Bangladesh was impacted by irradiance, mass flow rate, and inflow temperature. On the basis of the contributions of the conclusions indicated above, the following suggestions for additional research have been made:

- By examining various solar cell configurations, the study work can be expanded.
- By incorporating PCM into this model, further research can be done using a PVT/PCM model.
- Water can be used as a working fluid in upcoming studies.
- Another variation of this structure is single/hybrid/ternary nanofluid -based PVT.
- Another extension might be a reduced system and sun-tracking of the PVT system.
- PVT research may take on a fresh perspective if it takes into account the current properties of PVT systems produced by various companies in various nations.

References

- [1] H. Fayaz, N.A. Rahima, M. Hasanuzzamana, A. Rivaia, and R. Nasrin, "Numerical and outdoor real time experimental investigation of performance of PCM based PVT system," *Solar Energy*, vol 179, pp. 135-150, 2019.
- [2] M. Ashikuzzaman, R. Nasrin, F.T. Zohora, and M.S. Hossain, "3D study of heat transfer based on PVT/PCM system," *AIP Publishing*, vol 120007, pp. 120007-1—120007-9, 2019.
- [3] M.S. Hossain, A.K. Pandey, J. Selvaraj, N.A. Rahim, M.M. Islam, and V.V. Tyagi, "Two side serpentine flow based photovoltaic-thermal-phase change materials (PVT-PCM) system: Energy, exergy and economic analysis," *Renewable Energy*, vol 136, pp. 1320-1336, 2019.
- [4] A.H.A. Al-Waeli, M.T. Chaichan, H.A. Kazem, K. Sopian, A. Ibrahim, S. Mat, and Md.H. Ruslan, "Comparison study of indoor/outdoor experiments of a photovoltaic thermal PV/T system containing SiC nanofluid as a coolant," *Energy*, vol 151, pp. 33-44, 2018.
- [5] M. Tian, Y. Khetib, S. Yan, M. Rawa, M. Sharifpur, G. Cheraghian, and A.A. Melaibari, "Energy, exergy and economics study of a solar/thermal panel cooled by nanofluid," *Case Studies in Thermal Engineering*, vol 28, pp. 1-13, 2021.
- [6] A. Salari, A. Kazemian, T. Ma, A. Hakkaki-Fard, and J. Peng, "Nanofluid based photovoltaic thermal systems integrated with phase change materials: Numerical simulation and thermodynamic analysis," *Energy Conversion and Management*, vol 205, pp. 1-12, 2020.
- [7] A.H. Pordanjani, S. Aghakhani, M. Afrand, M. Sharifpur, J.P. Meyer, H. Xu, H.Md. Ali, N. Karimi, and G. Cheraghian, "Nanofluids: Physical phenomena, applications in thermal systems and the environment effects- a critical review," *Journal of Cleaner Production*, vol 320, pp. 1-38, 2021.

- [8] K. Hasan, S.B. Yousuf, Md.S.H.K. Tushar, B.K. Das, P. Das, and Md.S. Islam, "Effects of different environmental and operational factors on the PV performance: A comprehensive review," *Energy Science & Engineering*, vol 10, pp. 656-675, 2021.
- [9] Chr. Lamnatou, and D. Chemisana, "Photovoltaic/thermal (PVT) systems: A review with emphasis on environmental issues," *Renewable Energy*, vol 105, pp. 270-287, 2017.
- [10] R. Hossain, A.J. Ahmed, S.Md.K.N. Islam, N. Saha, P. Debnath, A.Z. Kouzani, and M.A.P. Mahmud, "New design of solar photovoltaic and thermal hybrid system for performance improvement of solar photovoltaic," *International Journal of Photoenergy*, vol 2020, pp. 1-6, 2020.
- [11] R. Alayi, F. Jahanbin, H.Ş. Aybar, M. Sharifpur, and N. Khalilpoor, "Investigation of the effect of physical factors on exergy efficiency of a photovoltaic thermal (PV/T) with air cooling," *International Journal of Photoenergy*, vol. 2022, pp. 1-6, 2022.
- [12] N.S.B. Rukman, A. Fudholi, I. Taslim, M.A. Indrianti, I.N. Manyoe, U. Lestari, and K. Sopian, "Electrical and thermal efficiency of air-based photovoltaic thermal (PVT) systems: An overview," *Indonesian Journal of Electrical Engineering and Computer Science*, vol. 14, pp. 1134-1140, 2019.
- [13] A. Fudholi, M.F. Musthafa, A. Ridwan, R. Yendra, A.P. Desvina, Rahmadeni, T. Suyono, and K. Sopian, "Energy and exergy analysis of air based photovoltaic thermal (PVT) collector: A review," *International Journal of Electrical and Computer Engineering (IJECE)*, vol. 9, pp. 109-117, 2018.
- [14] Q.A. Abed, V. Badescu, and I. Soriga, "Performance of a hybrid solar collector system in days with stable and less stable radiative regime," *International Journal of Sustainable Engineering*, vol. 11, pp. 40-53, 2018.
- [15] S.M. Sultan, and M.N.E. Efzan, "Review on recent photovoltaic/thermal (PV/T) technology advances and applications," *Solar Energy*, vol. 173, pp. 939-954, 2018.
- [16] M. Atmaca, and I.Z. Pektemir, "An investigation on the effect of the total efficiency of water and air used together as a working fluid in the photovoltaic thermal systems," *Processes*, vol. 7, 516, pp. 1-19, 2019.

- [17] A. Ghellab, T.E. Boukelia, S. Djimli, and A. Kaabi, "Numerical study of a hybrid photovoltaic/thermal PVT solar collector using three different fluids," *International Journal of Energetica (IJECA)*, vol. 6, pp. 55-56, 2021.
- [18] B. Das, B. Rezaie, P. Jha, and R. Gupta, "Performance analysis of single glazed solar PVT air collector in the climatic condition of NE India," *The 4th International Electronic Conference on Entropy and Its Applications (ECEA 2017)*, vol. 4, pp. 1-14, 2017.
- [19] J.C. Mojumder, W.T. Chong, H.C. Ong, K.Y. Leong, and A.A. Mamoon, "An experimental investigation on performance analysis of air type photovoltaic thermal collector system integrated with cooling fins design," *Energy and Buildings*, vol. 130, pp. 272-285, 2016.
- [20] R. Nasrin, M. Hasanuzzaman, and N.A. Rahim, "Effect of high irradiation and cooling on power, energy and performance of a PVT system," *Renewable Energy*, vol. 116, pp. 552-569, 2018.
- [21] Chr. Lamnatou, R.Vaillon, S. Parola, and D. Chemisana, "Photovoltaic/thermal systems based on concentrating and non-concentrating technologies: Working fluids at low, medium and high temperatures," *Renewable and Sustainable Energy Reviews*, vol. 137, pp. 1-61, 2021.
- [22] F.T. Zohora, and R. Nasrin, "A numerical analogy of improving efficiency for the PVT system in Bangladesh," *International Journal of Photoenergy*, vol. 2022, pp. 1-21, 2022.
- [23] R. Nasrin, and M.S. Hossain, "Numerical analysis of photovoltaic power generation in different locations of Bangladesh," *Journal of Computational and Applied Research in Mechanical Engineering*, vol. 10, pp. 373-389, 2021.
- [24] H. Fayaz, N.A. Rahim, M. Hasanuzzaman, R. Nasrin, and A. Rivai, "Numerical and experimental investigation of the effect of operating conditions on performance of PVT and PVT-PCM," *Renewable Energy*, vol. 143, pp. 827-841, 2019.

- [25] R. Nasrin, M. Hasanuzzaman, and N.A. Rahim, "Effect of nanofluids on heat transfer and cooling system of the photovoltaic/thermal performance," *International Journal of Numerical Methods for Heat Transfer and Fluid Flow*, vol. 29, pp. 1920-1946, 2019.
- [26] H. Fayaz, R. Nasrin, N.A. Rahim, and M. Hasanuzzaman, "Energy and exergy analysis of the PVT system: Effect of nanofluid flow rate," *Solar Energy*, vol. 169, pp. 217-230, 2018.
- [27] R. Nasrin, N.A. Rahim, H. Fayaz, and M. Hasanuzzaman, "Water/MWCNT nanofluid based cooling system of PVT: Experimental and numerical research," *Renewable Energy*, vol. 121, pp. 286-300, 2018.
- [28] R. Nasrin, M. Hasanuzzaman, and N.A. Rahim, "Effect of high irradiation on photovoltaic power and energy," *International Journal of Energy Research*, vol. 42, pp. 1115-1131, 2018.
- [29] M.M. Rahman, M. Hasanuzzaman, and N.A. Rahim, "Effects of operational conditions on the energy efficiency of photovoltaic modules operating in Malaysia," *Journal of Cleaner Production*, vol. 143, pp. 912-924, 2017.
- [30] O.C. Zienkiewicz, and R.L. Taylor, "The finite element method," Fourth Edition, McGraw-Hill, 1991.
- [31] R. Nasrin, "A 3D numerical study of thermo-fluid characteristics of a flat plate solar collector using nanofluid," Ph.D. Thesis, Department of Mathematics, Bangladesh University of Engineering and Technology, Dhaka, Bangladesh, 2015.
- [32] M. Chandrasekar, S. Suresh, T. Senthilkumar, and M.G. Karthikeyan, "Passive cooling of standalone flat PV module with cotton wick structures," *Energy Conversion and Management*, vol. 71, pp. 43-50, 2013.
- [33] H. Bahaidarah, A. Subhan, P. Gandhidasan, and S. Rehman, "Performance evaluation of a PV (photovoltaic) module by back surface water cooling for hot climatic conditions," *Energy*, vol. 59, pp. 445-453, 2013.